

# **Maison de la Riviere**

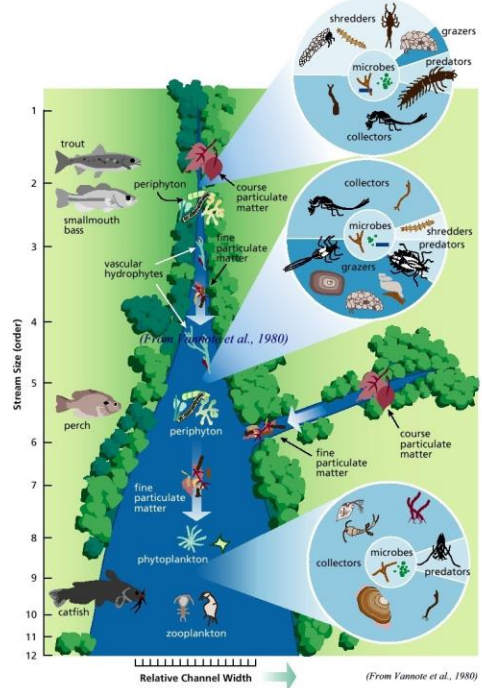
06 May 08:30 departure – return 14:00

The bus will be waiting Av. Piccard, vis-à-vis from Négoce

Check weather please and show up dressed accordingly

Bring your lunch box

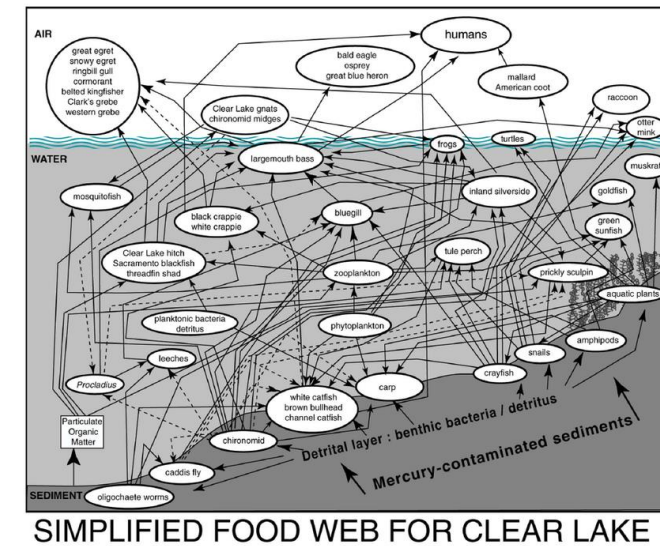
## River Continuum Concept



## Spatial heterogeneity and community metabolism

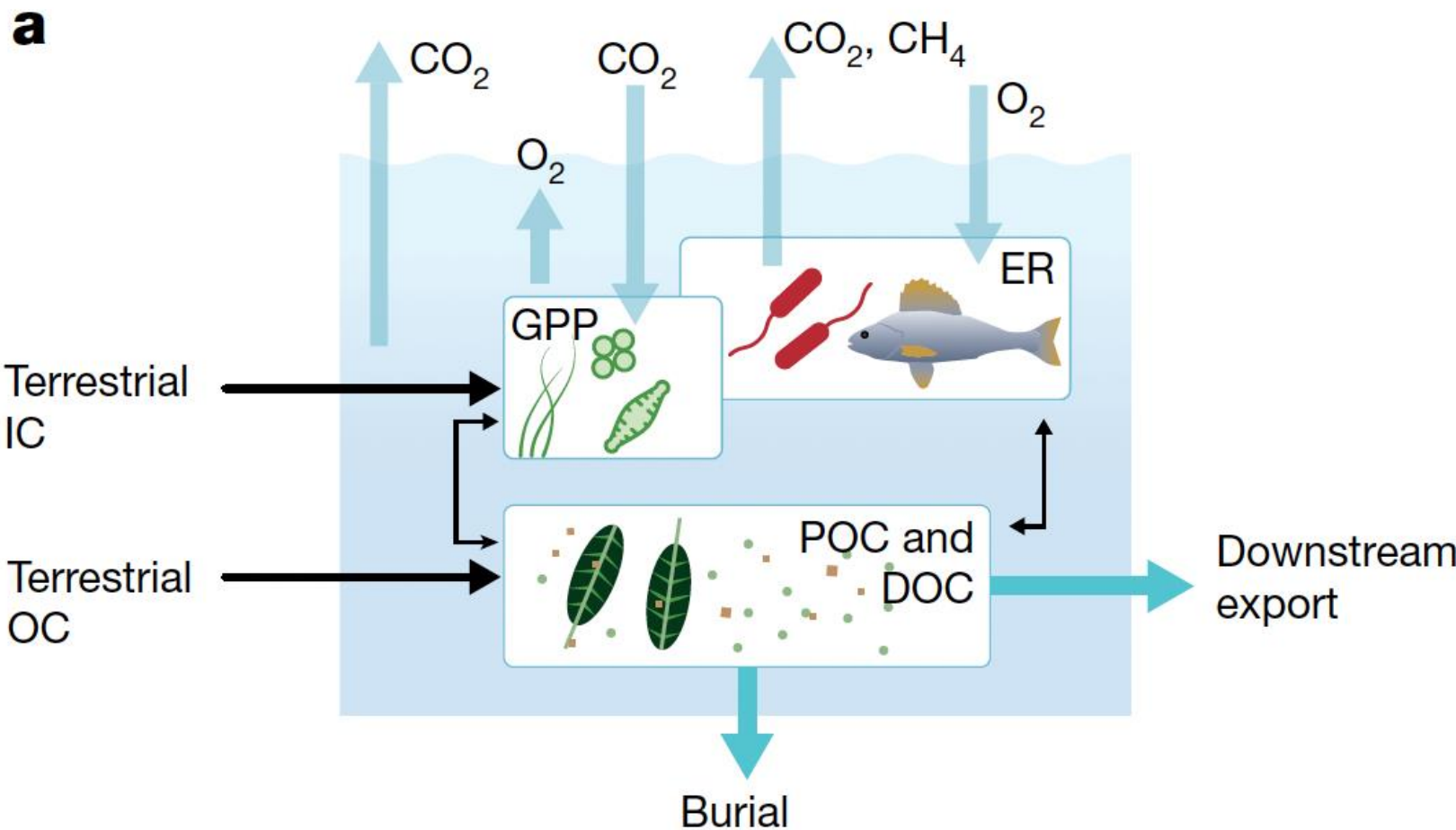


## Food webs



# Ecosystem metabolism

**Ecosystem metabolism as the sum of the production and respiration of all organisms with an ecosystem, regulating major ecosystem carbon fluxes**



**Integrates metabolic fluxes with carbon and nutrient dynamics in stream and river ecosystems**

Primary Production in Flowing Waters<sup>1</sup>

HOWARD T. ODUM

Department of Zoology, Duke University, Durham, N. C.

## ABSTRACT

Respiration, photosynthetic production, and diffusion interact to produce the daily curve of oxygen change in a segment of flowing water. Conversely, the observed curves of oxygen in streams can be used to calculate the component rates of production, respiration, and diffusion. New production values obtained with these analyses of oxygen curves from various sources, as well as a few previously existing estimates of primary production, indicate a generally higher rate of production in flowing waters than in other types of aquatic environments.

The ratio of total primary production to total community respiration is used to classify communities quantitatively according to their predominantly heterotrophic or autotrophic characteristics. Longitudinal succession within a stream tends to modify the ratio towards unity from higher values for autotrophic and from lower values for heterotrophic communities. The behavior of this ratio is described for the annual cycle in a stream, for the sequence of pollution recovery, and for diverse types of communities.

## INTRODUCTION

To the casual eye the biota of flowing waters is rich. Coral reefs, river rapids, tidal channels, and the lush plant beds of calcareous streams seem to be full of life. In the polluted Illinois River, almost unbelievable concentrations of bottom organisms have been found. How are such communities supported? What is the magnitude of primary production in comparison to other communities? How does the dominating current-flow relate to other energy-flows through the communities?

ments of production very simple in flowing water. The task here, therefore, is to re-evaluate some of the extensive information on flowing waters in terms of productivity and community respiration especially by using diurnal gas curves and the upstream-downstream method of measuring community metabolism. A summary will then be made of the production and respiration of flowing communities relative to succession, velocity of current, and the classification of communities.

## THEORETICAL CONSIDERATION OF DAILY PROCESSES OF OXYGEN METABOLISM IN FLOWING WATERS

Consider a stretch of flowing water delimited by two stations, one upstream from the other. During the usual daily cycle four main processes affect the oxygen and carbon-dioxide concentrations of water flowing between the stations. Although the discussion here is presented in terms of oxygen, it should be understood that carbon dioxide behaves similarly but with reversed sign.

(1) There is a release of oxygen into the water as a result of photosynthetic primary production during the day by both benthic plants and phytoplankton.

(2) There is an uptake of oxygen from the water as a result of the respiration of benthic

## PRIMARY PRODUCTION IN FLOWING WATERS

113

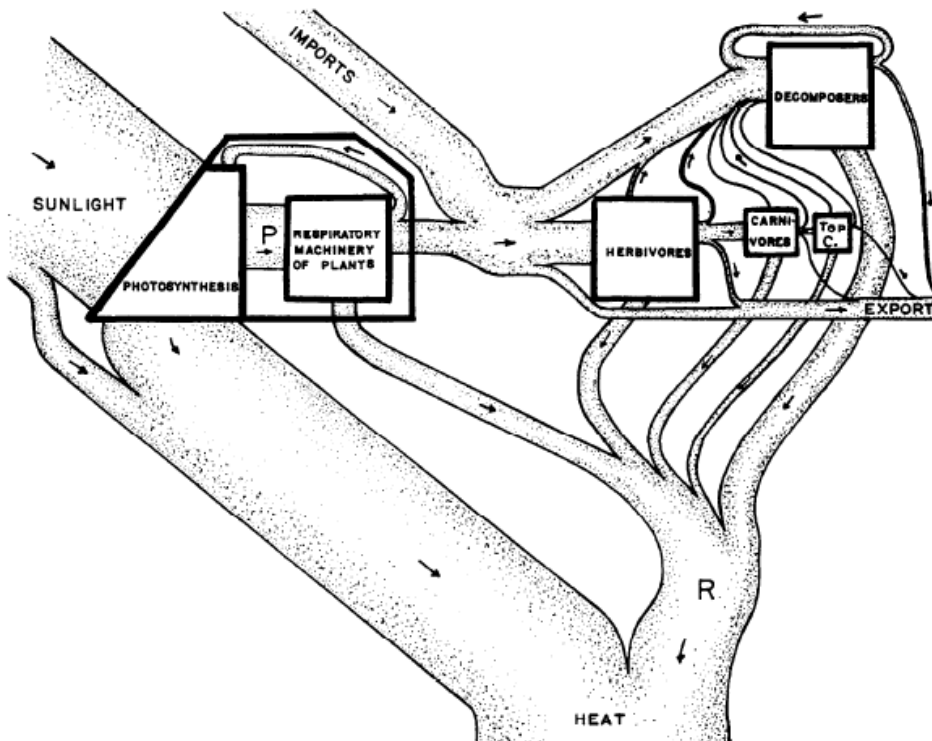
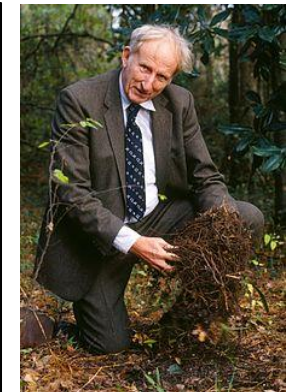


FIG. 6. A generalized diagram of energy flow for steady state natural communities.  $P$  is the gross primary production;  $R$  is the total community respiration; the 5 trophic levels are indicated by boxes. Imports and exports are included as dominant flows which may equal the flow of primary production in some streams. The flow from the top of those boxes representing consumer trophic levels indicates unassimilated materials. The laws of thermodynamics are illustrated since inflows balance outflows and every process is accompanied by dispersion of heat energy as entropy tax.



## Revisiting Odum (1956): A synthesis of aquatic ecosystem metabolism

Timothy J. Hoellein,<sup>1,\*</sup> Denise A. Bruesewitz,<sup>2</sup> and David C. Richardson<sup>3</sup>

Most streams and rivers consume more organic carbon (respiration; ER) than they produce (primary production; GPP)

They are net heterotrophic, that means  $ER > GPP$  ( $NEP < 0$ )

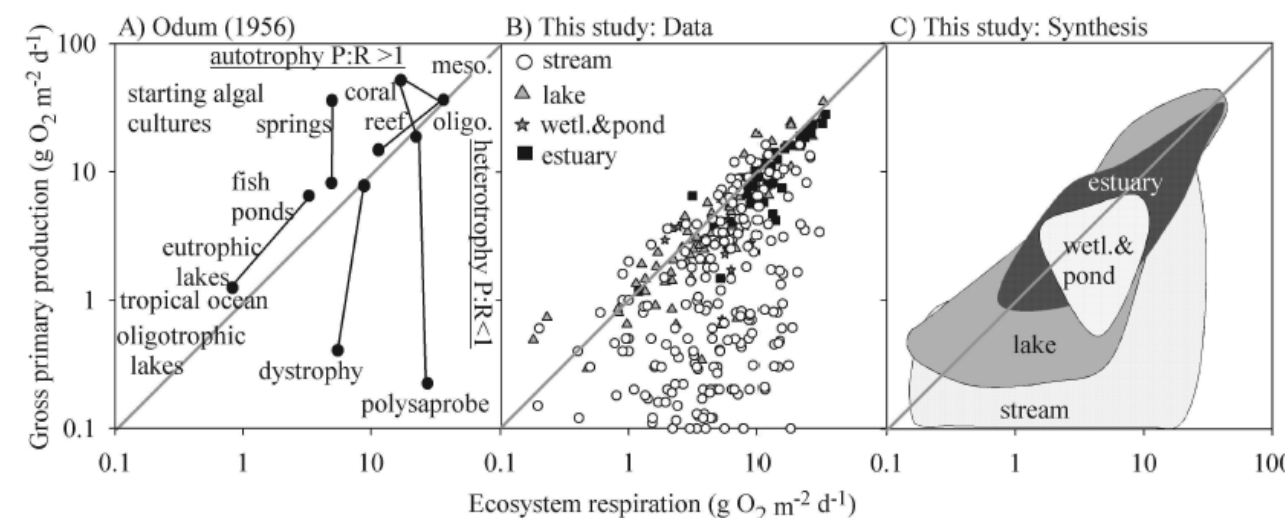


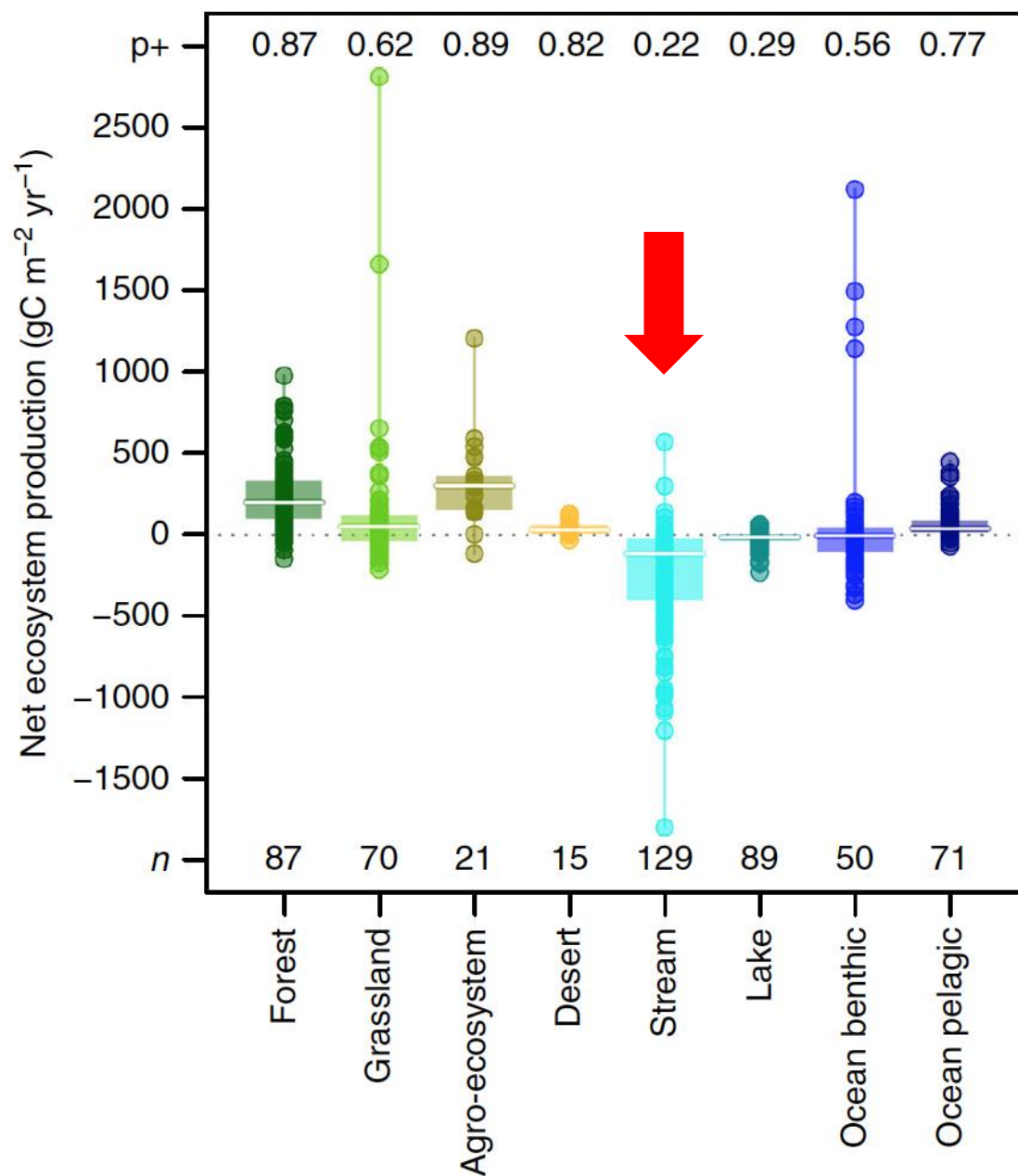
Fig. 1. (A) Odum's (1956) synthesis of metabolism measurements across aquatic ecosystems. Points connected by lines were taken within the same site; meso = mesosaprobe; oligo = oligosaprobe. (B) Our synthesis of data from open-water measurements of metabolism in streams, lakes, wetlands and ponds, and estuaries using identical graphical framework and axes to those in Odum (1956), and (C) a plot of the two-dimensional area that encompasses all data points for each of the four ecosystem types. The gray line indicates 1:1 value of GPP:ER on each panel (Odum 1956).

# Cross-ecosystem carbon flows connecting ecosystems worldwide

Isabelle Gounand  <sup>1,2</sup>, Chelsea J. Little  <sup>1,2</sup>, Eric Harvey  <sup>1,2,3</sup> & Florian Altermatt  <sup>1,2</sup>

Streams and rivers belong to the most heterotrophic ecosystems

**Fig. 4** Net ecosystem production for different ecosystem types. Net ecosystem production (NEP) corresponds to the balance between gross primary production and ecosystem respiration. Negative values denote net heterotrophic functioning. Circles give individual values in  $\text{gC m}^{-2} \text{ year}^{-1}$ . Note that these are production fluxes and not productivity rates (biomass turnover), for which we would have higher values in aquatic compared to terrestrial ecosystems. Boxplots give median (white line), 25 and 75% percentiles (box), and range (whiskers). Top numbers ( $p+$ ) give the probability of NEP being positive within each ecosystem type, assuming normal distributions of the data (quantile corresponding to 0). Bottom numbers ( $n$ ) indicate the number of data points. The 95% confidence intervals for mean NEP within each ecosystem types are in  $\text{gC m}^{-2} \text{ year}^{-1}$ : Forest [204; 301], Grassland [28; 224], Agro-ecosystem [197; 438], Desert [18; 70], Stream [-307; -193], Lake [-32; -14], Ocean benthic [-60; 201], and Ocean pelagic [47; 90] (see full results of two-sided  $t$ -test in Supplementary Table 1). A conservative non-parametric Kruskal-Wallis' test indicates significant differences among ecosystems ( $\chi^2_{7,532} = 275.04, P < 0.001$ ). The post-hoc multiple comparisons test using rank sums gives the following groups: a, bc, a, abcd, e, d, bd, ac (lower case letters for grouping from left to right in the figure; see Methods)

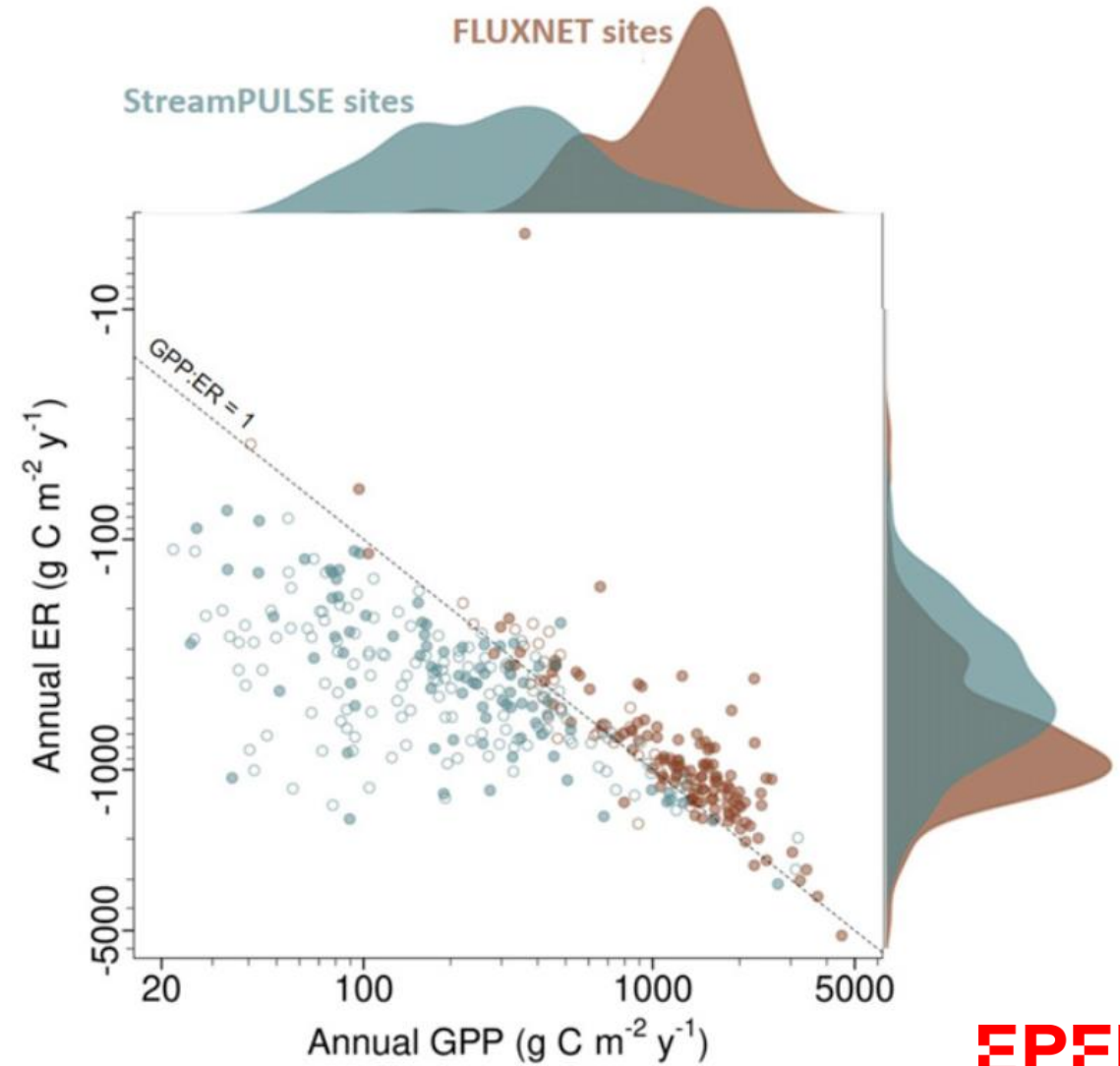


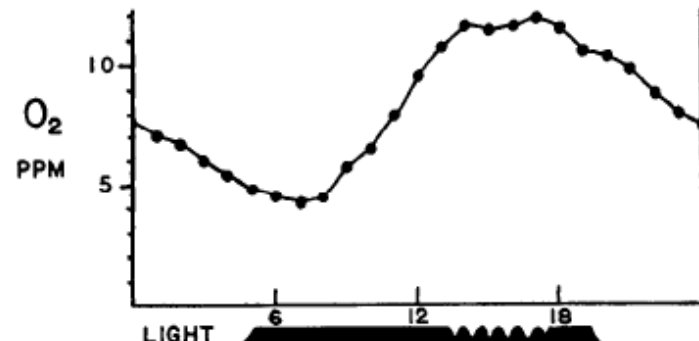
# Light and flow regimes regulate the metabolism of rivers

Emily S. Bernhardt<sup>a,1,2</sup>, Phil Savoy<sup>a,b,1</sup>, Michael J. Vlah<sup>a</sup>, Alison P. Appling<sup>c</sup>, Lauren E. Koenig<sup>c,d,e</sup>, Robert O. Hall Jr.<sup>e</sup>, Maite Arroita<sup>f</sup>, Joanna R. Blaszczak<sup>e,g</sup>, Alice M. Carter<sup>a,c</sup>, Matt Cohen<sup>a</sup>, Judson W. Harvey<sup>c</sup>, James B. Heffernan<sup>i</sup>, Ashley M. Helton<sup>d,j</sup>, Jacob D. Hosen<sup>k</sup>, Lily Kirk<sup>b</sup>, William H. McDowell<sup>l</sup>, Emily H. Stanley<sup>m</sup>, Charles B. Yackulic<sup>n</sup>, and Nancy B. Grimm<sup>a,2</sup>

Annual regimes of river metabolism show their higher heterotrophy (ER>>GPP) compared to terrestrial ecosystems

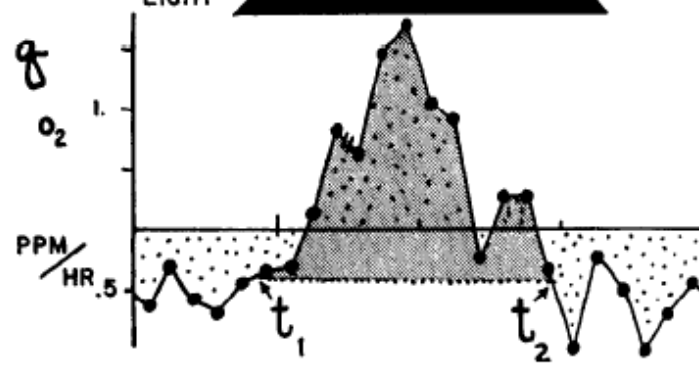
**Fig. 1.** Annual rates of GPP and ER for 222 river and 162 terrestrial ecosystems are shown as a scatterplot relative to the 1:1 line of balanced aerobic ecosystem carbon production and consumption. The frequency distribution of GPP and ER values within each dataset is shown above and to the right of the scatterplot, with values aligned to the corresponding axis. Open circles indicate sites with at least 60% of all days in each year having estimated rates, and solid circles indicate sites with at least 80% of all days in each year having estimated rates. We show average annual values for sites with multiple years.





## Diel Oxygen Curves

- Gross Primary Production
- Ecosystem Respiration
- Gas exchange with atmosphere driven by diffusion



Production of oxygen

Consumption of oxygen

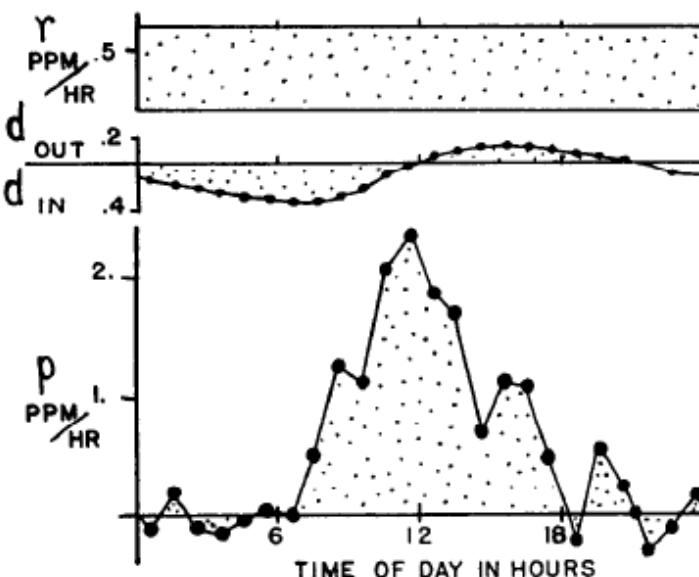
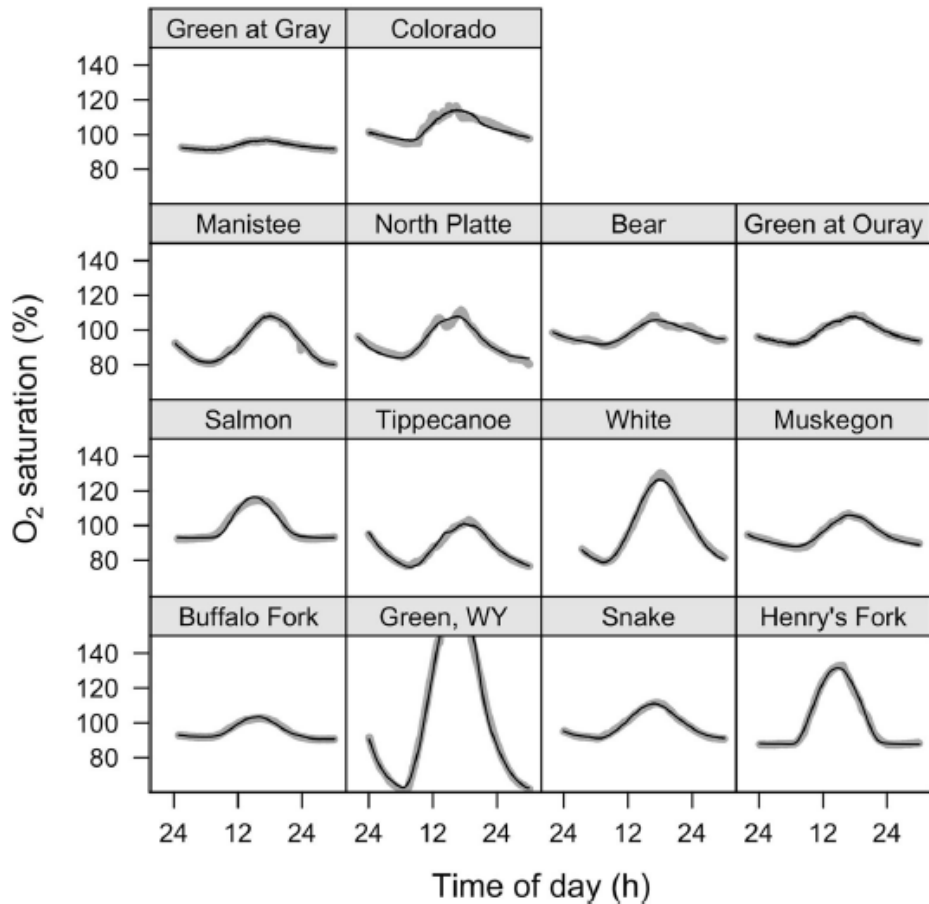


FIG. 3. Component processes in ppm/hr in the daily oxygen metabolism of the River Lark, England, calculated by the single-curve method from data given by Butcher, Pentelow, and Woodley (1930). In the upper curve is given the observed diurnal (24-hr) oxygen curve. From this is calculated the rate of change per hour in ppm/hr ( $q$ ). Respiration ( $r$ ), diffusion ( $d$ ), and production ( $p$ ) on a ppm-basis are calculated as indicated in the text on the assumption that the stream is homogeneous. The shaded area delimited by  $t_1$  and  $t_2$  is used in Equation (5) to determine the approximate production uncorrected for diffusion.



# Metabolism, Gas Exchange, and Carbon Spiraling in Rivers

Robert O. Hall Jr.,<sup>1,\*</sup> Jennifer L. Tank,<sup>2</sup> Michelle A. Baker,<sup>3</sup>  
Emma J. Rosi-Marshall,<sup>4</sup> and Erin R. Hotchkiss<sup>5,6</sup>



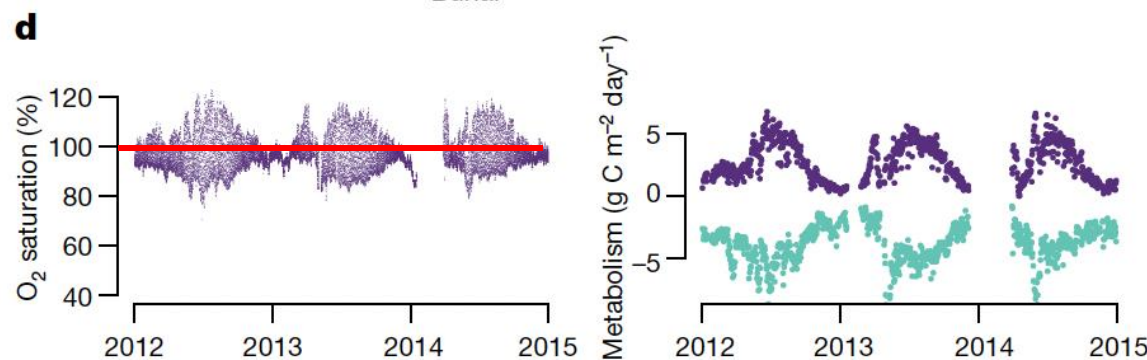
## Estimating whole-ecosystem metabolism

$$\frac{dO}{dt} = \frac{GPP}{z} + \frac{ER}{z} + K(O_{sat} - O)$$

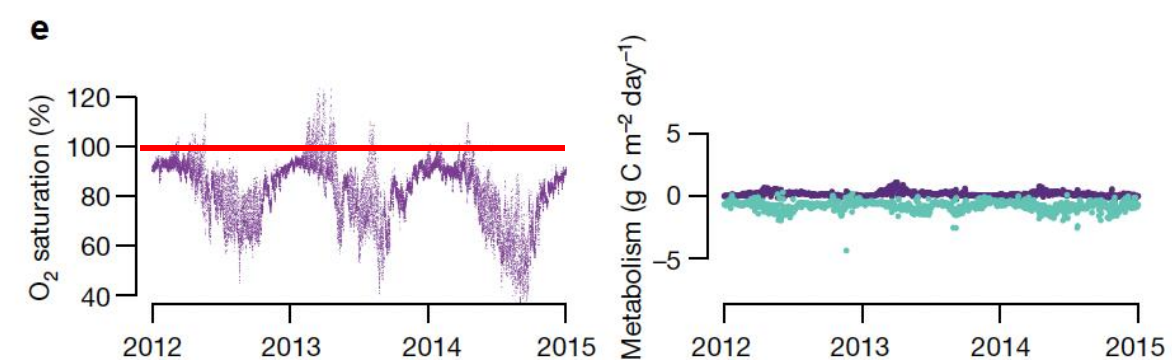
- Dissolved oxygen (O)
- Dissolved oxygen (at saturation)
- GPP, ER
- Depth (z)
- Gas exchange rate (K), depends on turbulence (slope, roughness, flow velocity)

# Time series of dissolved oxygen to daily GPP and ER

Productive stream



Unproductive stream



## The metabolic regimes of flowing waters

E. S. Bernhardt <sup>1</sup>\*, J. B. Heffernan <sup>2</sup>, N. B. Grimm <sup>3</sup>, E. H. Stanley <sup>4</sup>, J. W. Harvey <sup>5</sup>,  
M. Arroita, <sup>6,7</sup> A. P. Appling, <sup>8</sup> M. J. Cohen, <sup>9</sup> W. H. McDowell <sup>10</sup>, R. O. Hall, Jr., <sup>7,a</sup> J. S. Read, <sup>11</sup>  
B. J. Roberts, <sup>12</sup> E. G. Stets, <sup>13</sup> C. B. Yackulic <sup>14</sup>

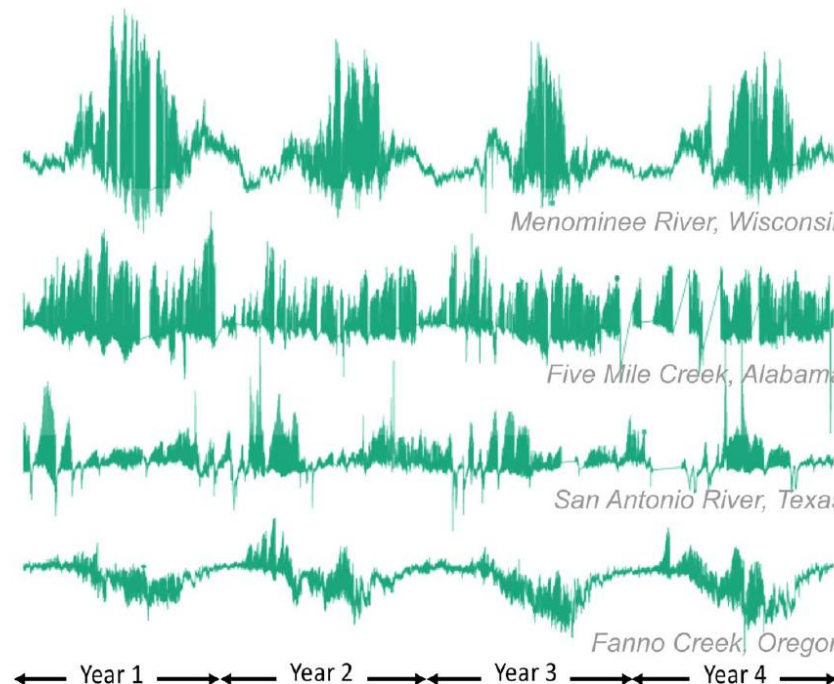


**Fig. 1.** Temporal trends in dissolved oxygen (DO shown as % of atmospheric saturation) for four contrasting U.S. rivers over a 4-yr period. High diel variation in dissolved oxygen is a proxy for high ecosystem GPP. The top trace is from the Menominee River in northern, Wisconsin, a large river with clear summer peaks and winter lows in stream metabolism. Dissolved oxygen traces for the more southern Five Mile Creek in Alabama and San Antonio River in Texas show little seasonality, with the smaller Creek having sustained high diel variation in DO and the more urban river having many alternating periods of high and low diel DO variation. The bottom trace is from Fanno Creek, a heavily shaded and frequently flooded small stream in western Oregon. Data from each of these four streams appears again (along with axes labels) in Figs. 3, 5. Here, we remove axes scores to focus on the differences in seasonality of a common signal across streams. The scale of both axes is the same for all four series. [Color figure can be viewed at [wileyonlinelibrary.com](http://wileyonlinelibrary.com)]

Large river, clear summer peaks,  
winter lows (phytoplankton?)

Little seasonality

Urban river

Heavily shaded, frequently flooded

## The metabolic regimes of flowing waters

E. S. Bernhardt <sup>1</sup>\*, J. B. Heffernan <sup>2</sup>, N. B. Grimm <sup>3</sup>, E. H. Stanley <sup>4</sup>, J. W. Harvey <sup>5</sup>,  
M. Arroita, <sup>6,7</sup> A. P. Appling, <sup>8</sup> M. J. Cohen, <sup>9</sup> W. H. McDowell <sup>10</sup>, R. O. Hall, Jr., <sup>7,a</sup> J. S. Read, <sup>11</sup>  
B. J. Roberts, <sup>12</sup> E. G. Stets, <sup>13</sup> C. B. Yackulic <sup>14</sup>

# Controls on ecosystem metabolism

- Light and nutrients
- Temperature
- Flow-induced abrasion and erosion of biomass

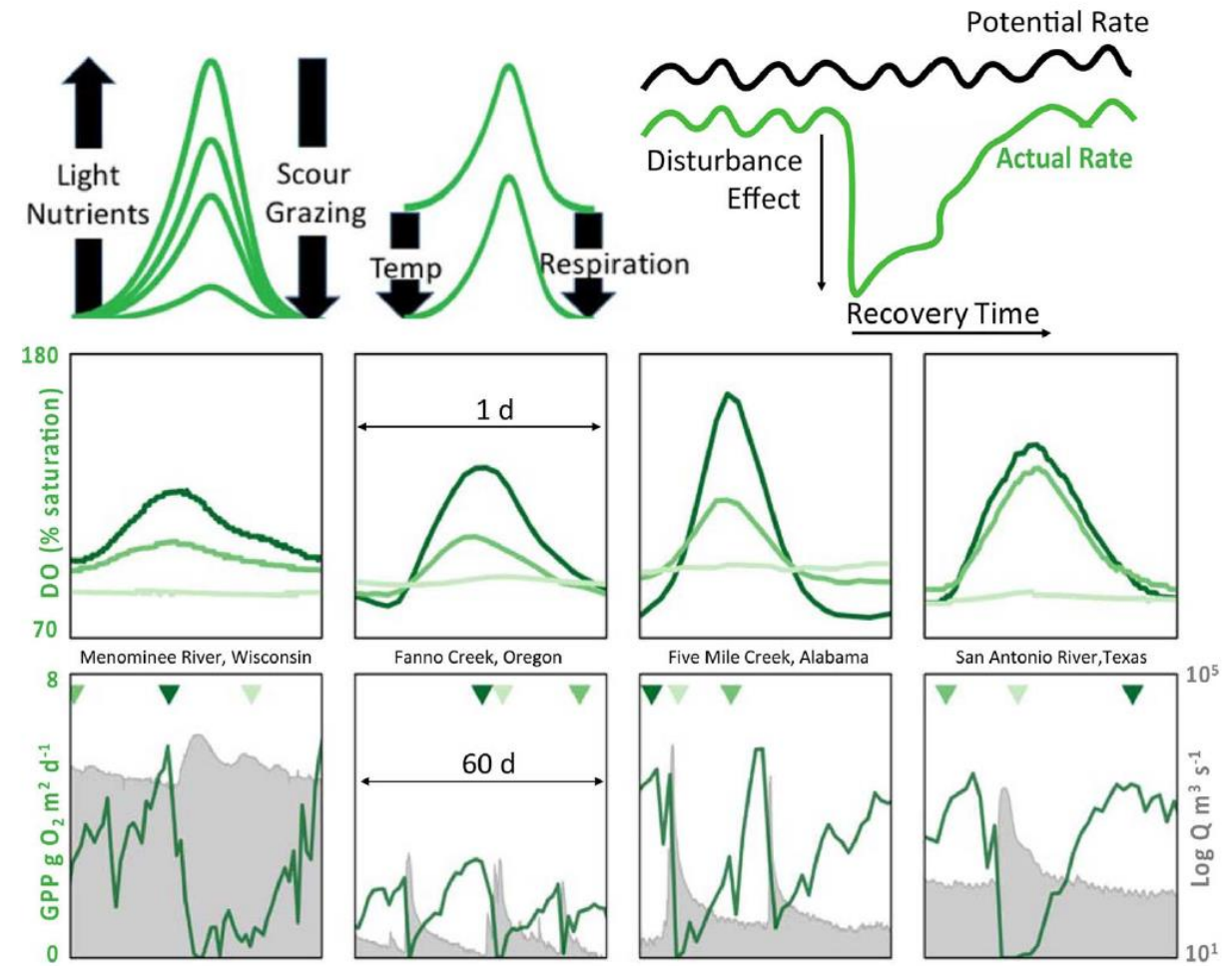
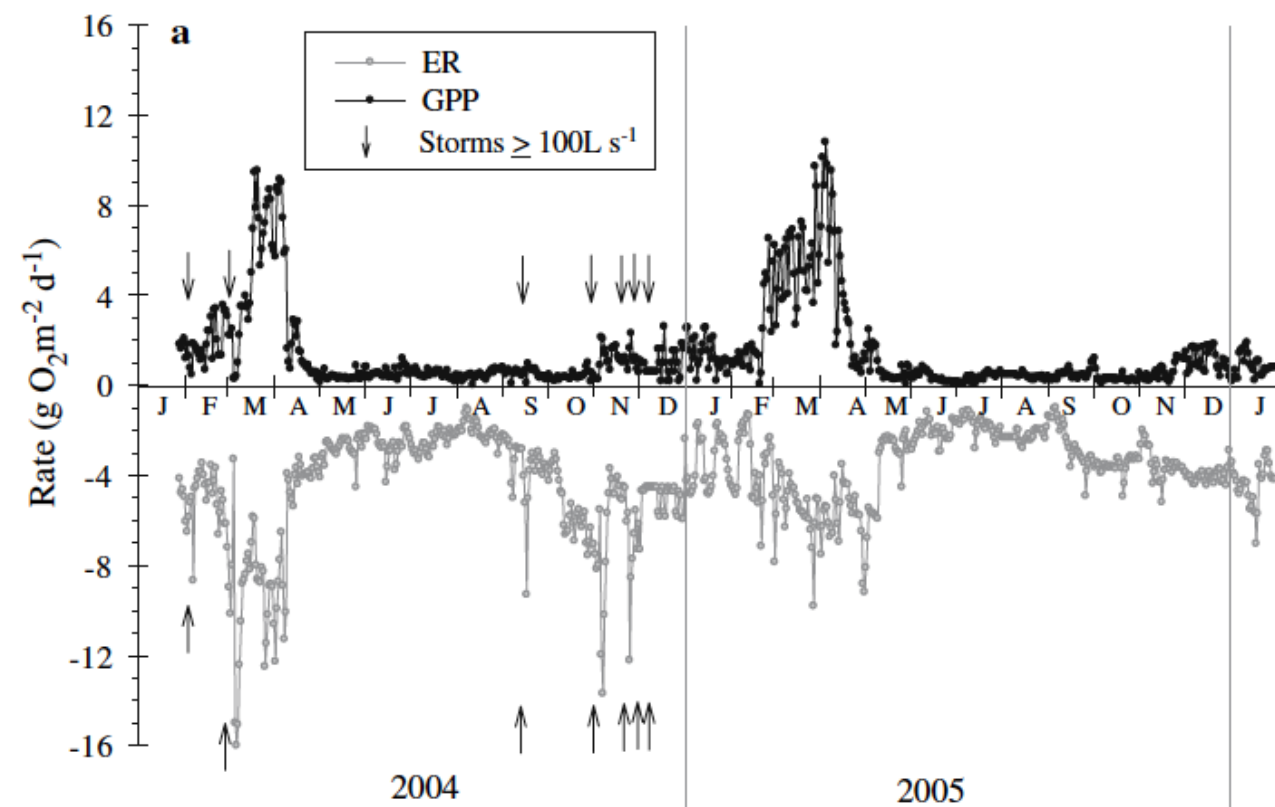


**Fig. 3.** Diel and Storm Recovery Patterns in Rivers. Figures in row A are conceptual models representing the typical variation in O<sub>2</sub> (as % saturation) at diel (A1, A2) and over storm-recovery trajectories (A3). Figures in row B show three contrasting diel curves selected from each of the four rivers shown in Fig. 1. In row C, we show 60 d of estimated rates of gross primary productivity (in green, derived from the O<sub>2</sub> data in Fig. 1) alongside the river hydrograph (gray shading). Each 60-d period encompasses at least one major flood. The color and date of the triangles shown at the top of panels in row C correspond to the dates for the diel O<sub>2</sub> curves shown in row B. [Color figure can be viewed at [wileyonlinelibrary.com](http://wileyonlinelibrary.com).]

# Multiple Scales of Temporal Variability in Ecosystem Metabolism Rates: Results from 2 Years of Continuous Monitoring in a Forested Headwater Stream

Brian J. Roberts,<sup>1,\*</sup> Patrick J. Mulholland,<sup>1</sup> and Walter R. Hill<sup>2</sup>

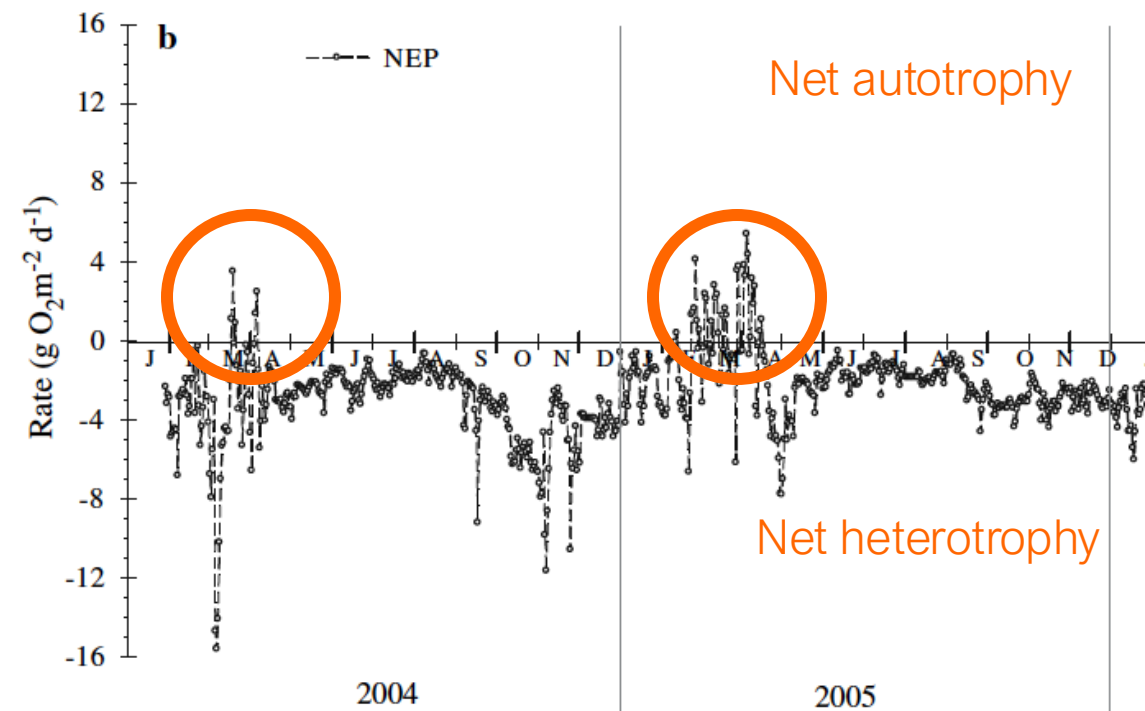
## What drives annual regimes of ecosystem metabolism?



## Multiple Scales of Temporal Variability in Ecosystem Metabolism Rates: Results from 2 Years of Continuous Monitoring in a Forested Headwater Stream

Brian J. Roberts,<sup>1,\*</sup> Patrick J. Mulholland,<sup>1</sup> and Walter R. Hill<sup>2</sup>

# What drives annual regimes of ecosystem metabolism?



Autotrophy ( $\text{GPP} > \text{ER}$ )

- Spring: algal blooms, little canopy, enough light
- Net sinks for atmospheric  $\text{CO}_2$

Net autotrophy

Net heterotrophy

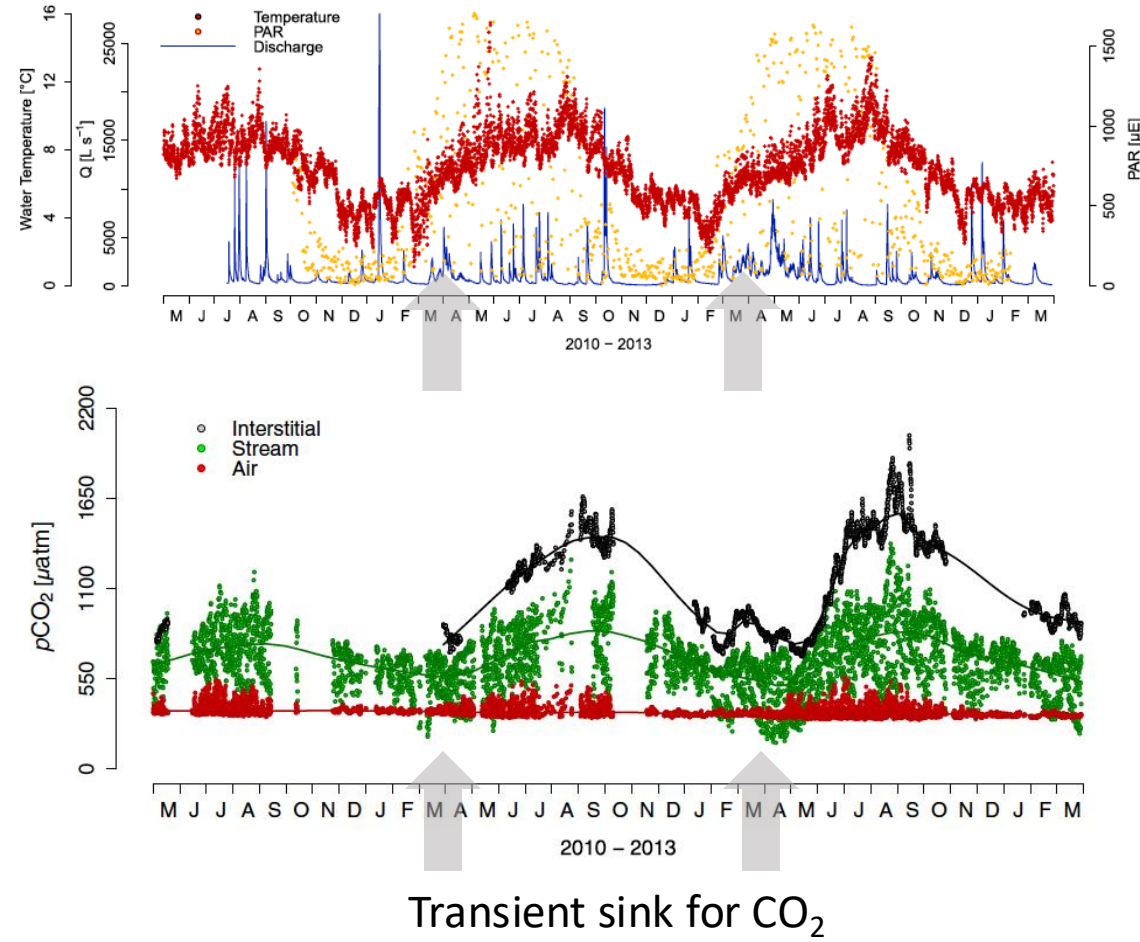
## RESEARCH ARTICLE

10.1002/2013JG002552

Scales and drivers of temporal  $p\text{CO}_2$  dynamics  
in an Alpine stream

Key Points:

- High temporal dynamics of  $p\text{CO}_2$  in streams

Hannes Peter<sup>1</sup>, Gabriel A. Singer<sup>2,3,4</sup>, Christian Preller<sup>3</sup>, Peter Chifflard<sup>5</sup>, Gertraud Steniczka<sup>3</sup>,  
and Tom J. Battin<sup>2,3</sup>

## Autotrophy (GPP &gt; ER)

- Net sinks for atmospheric  $\text{CO}_2$
- Spring: algal blooms draw down  $\text{CO}_2$

# Multiple Scales of Temporal Variability in Ecosystem Metabolism Rates: Results from 2 Years of Continuous Monitoring in a Forested Headwater Stream

Brian J. Roberts,<sup>1,\*</sup> Patrick J. Mulholland,<sup>1</sup> and Walter R. Hill<sup>2</sup>

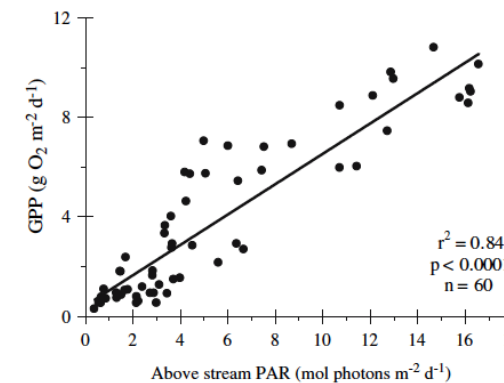


Figure 6. Relationships between daily gross primary production (GPP) rate and daily integrated photosynthetically active radiation (PAR) flux measured 1m above the stream surface during the period of peak autotrophic biomass (April 2004 and 2005,  $n = 60$ ). Solid line is the statistically significant ( $P < 0.0001$ ) linear regression ( $GPP = 0.61 \times (PAR) + 0.43$ ).

- Seasonal patterns (light, temperature...)
- Event-driven patterns (scouring...)

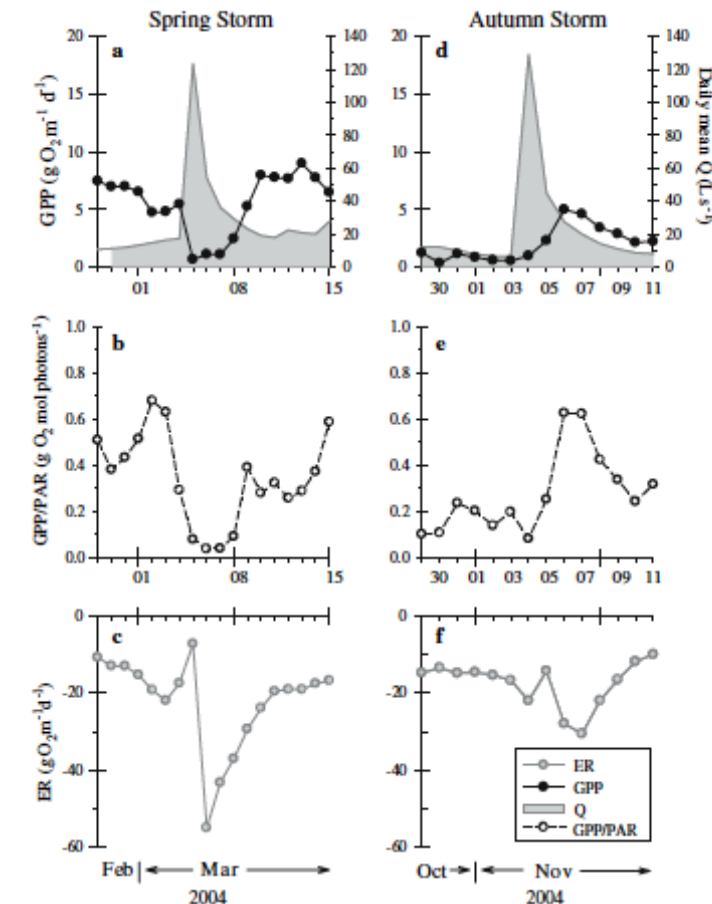


Figure 7. Daily rates of gross primary production (GPP, A, D), photosynthetic efficiency (GPP/PAR, B, E), and ecosystem respiration (ER, C, F) before and after large spring (A, B, C) and autumn (D, E, F) storms in 2004. Daily  $Q$  is indicated as the shaded area in panels A and B for the spring and autumn storms, respectively.

## Continuous monitoring reveals multiple controls on ecosystem metabolism in a suburban stream

JAKE J. BEAULIEU\*, CLAY P. ARANGO†, DAVID A. BALZ‡ AND WILLIAM D. SHUSTER\*

- Photosynthetic active radiation and inhibition (see also lakes) of photosynthesis rates
- Higher biomass prior to the storm resulting in higher GPP

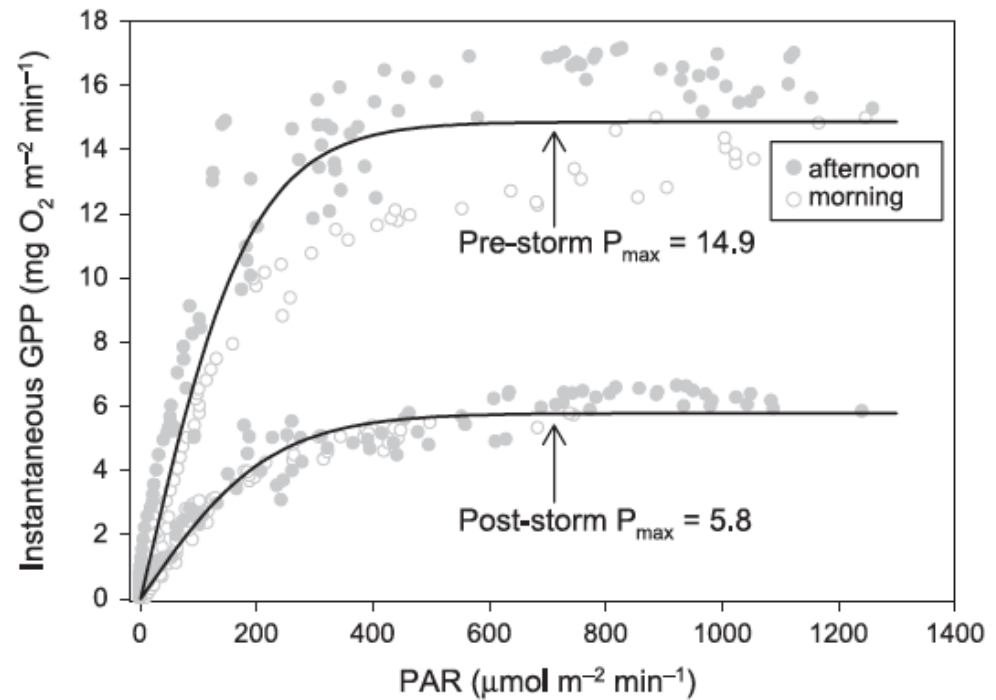
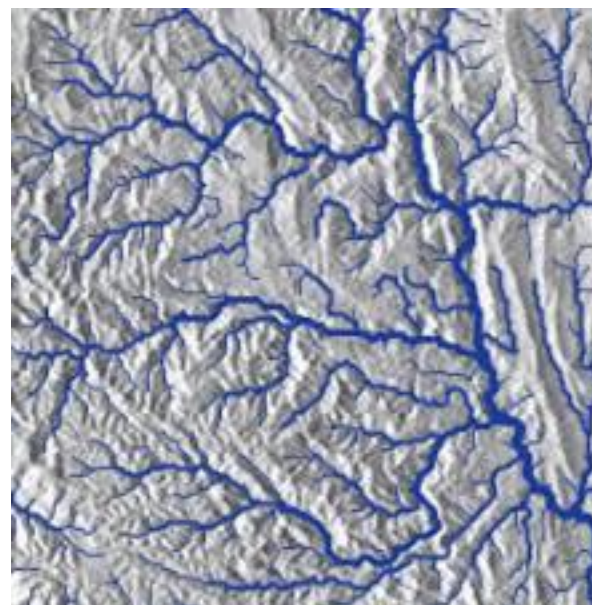


Fig. 7 Photosynthesis–irradiance curves on 3 April and 6 April 2011. Storm flows exceeding  $1400 \text{ L s}^{-1}$  occurred during the intervening 2 days. Pre- and post-storm maximum photosynthesis rates ( $P_{\max}$ ) are indicated. Open and filled circles represent morning and afternoon hours, respectively. The pre-storm data exhibit counterclockwise hysteresis. No hysteresis is apparent in the post-storm data.

# **Ecosystem metabolism**

From stream reaches to the network

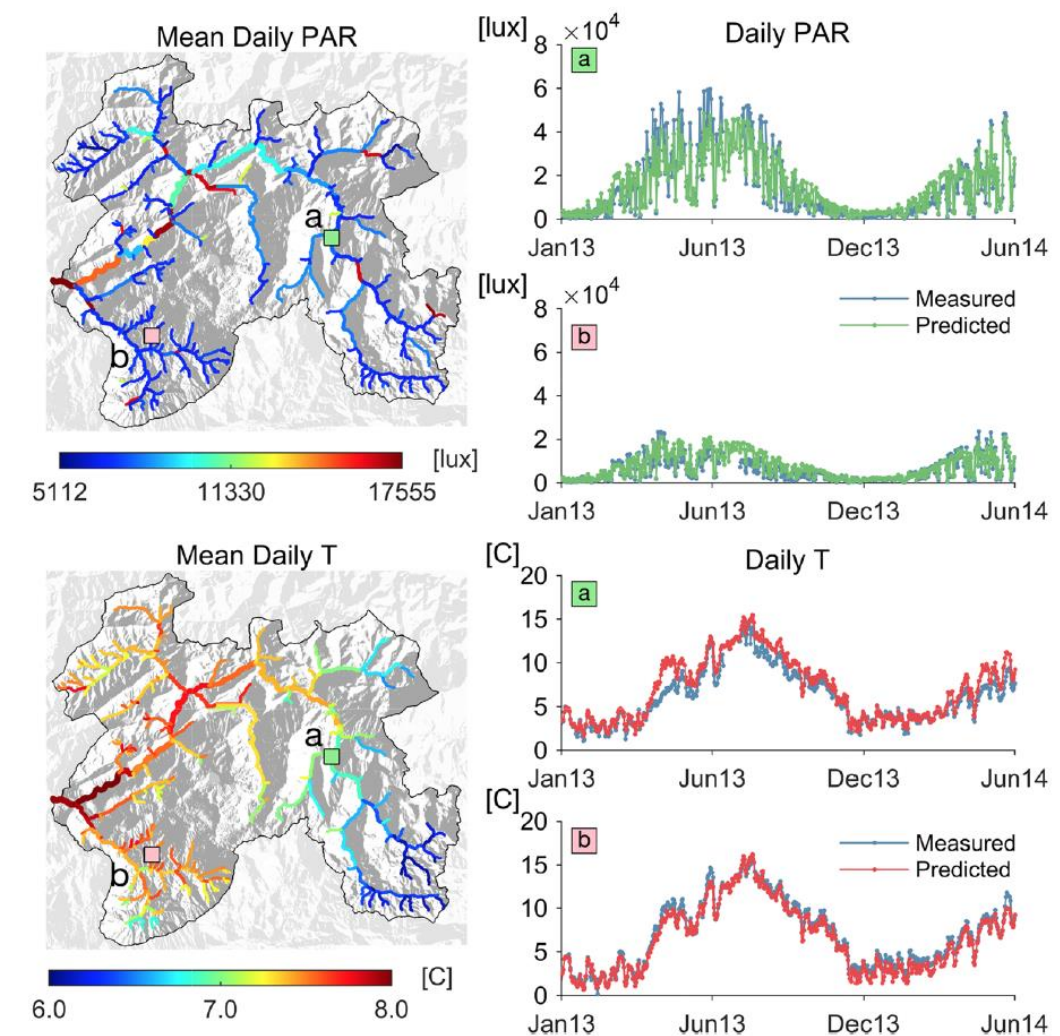


# The Metabolic Regimes at the Scale of an Entire Stream Network Unveiled Through Sensor Data and Machine Learning

Pier Luigi Segatto,<sup>1</sup> Tom J. Battin,<sup>1\*</sup> and Enrico Bertuzzo<sup>2\*</sup>

## Using machine learning to predict annual regimes of the drivers of GPP and ER at network scale

Figure 2. Random forest (RF) predictions of light (PAR) and streamwater temperature (T). Maps in the left column show RF predictions for mean daily PAR (top) and streamwater temperature (bottom) of the 292 stream reaches composing the Ybbs river network. Plots in the right column show the comparison between the time series of measured and predicted mean daily PAR and T for two representative reach sites (a and b, see location on the maps). The comparison for the remaining sites is reported in SI Results in Figures S23 and S25. Results refer to the S training (see “[Methods](#)” section). The predicted time series reported here are derived using the RFs trained excluding the site shown (that is, site a and b, respectively). Maps show the results of the ensemble RF, that is, the average of the 12 RFs obtained excluding all sites one at a time (see “[Methods](#)” section).



# The Metabolic Regimes at the Scale of an Entire Stream Network Unveiled Through Sensor Data and Machine Learning

Pier Luigi Segatto,<sup>1</sup> Tom J. Battin,<sup>1\*</sup> and Enrico Bertuzzo<sup>2\*</sup>

- Predicting annual regimes of GPP, ER and NEP at network scale
- According to the RCC, more heterotrophy (i.e., more negative NEP) in the headwaters
- Why would this be so?

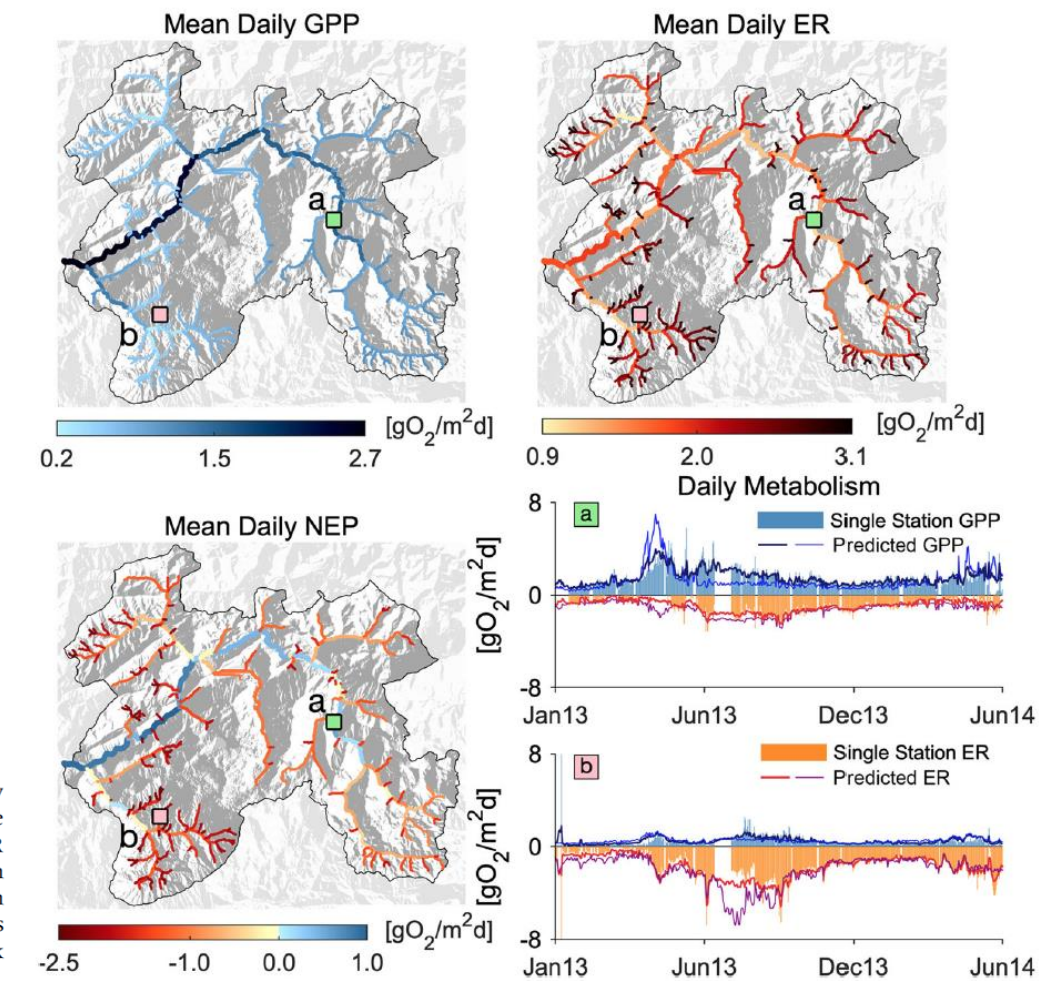
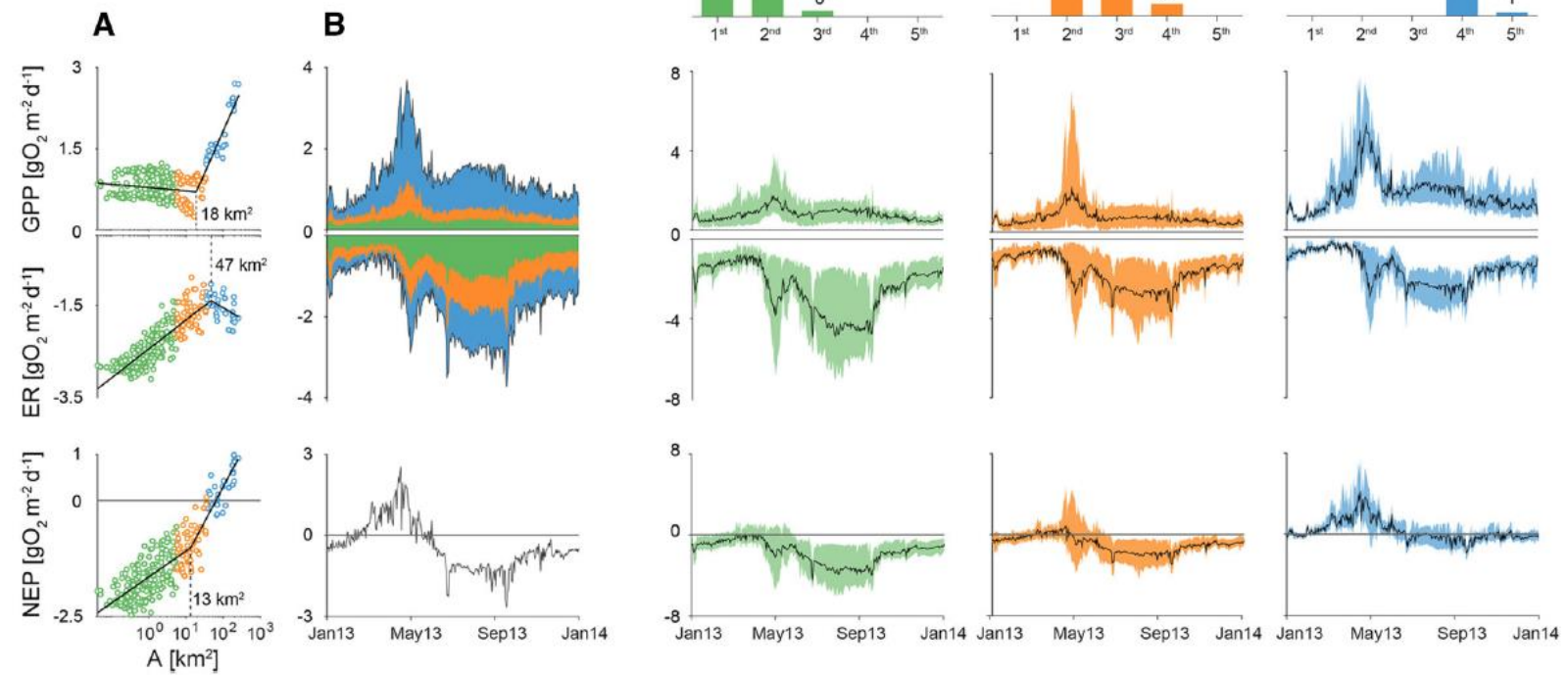


Figure 3. Random Forest (RF) predictions of network-scale metabolic regimes. Maps show RF predictions for mean daily GPP (top-left) and ER (top-right), and NEP (bottom-left) as difference between GPP and ER. Plots (bottom-right) show the comparison between the time series of estimated (via the single-station approach) and predicted (via RF) daily GPP and ER for two representative reach sites (a and b, see location on the maps). The comparison for the remaining sites is reported in SI Results in Figure S27. Results refer to the RF trained in the S setup and that does not include the predicted PAR and T in the feature library (see “Methods” section). Maps show the results of the ensemble RF, that is the average of the 12 RFs obtained excluding all sites one at a time (see “Methods” section). Plots report both the prediction of the ensemble RF (thick line) and of the RF trained excluding the site shown (thin line).

# The Metabolic Regimes at the Scale of an Entire Stream Network Unveiled Through Sensor Data and Machine Learning

Pier Luigi Segatto,<sup>1</sup> Tom J. Battin,<sup>1\*</sup> and Enrico Bertuzzo<sup>2\*</sup>

- Pronounced heterotrophy in the headwaters
- Pronounced spring peak of GPP in the lower reaches, shaping network metabolism



**Figure 4.** Stream ecosystem metabolic regime at network scale. Stream reaches have been clustered in three major groups according to their Strahler's stream order and catchment size (panel a and c). Group I (green) includes all streams with catchment size smaller than the largest first-order stream ( $5.6 \text{ km}^2$ ), group II (orange) those smaller than the largest third-order stream (that is, from  $5.6$  to  $36 \text{ km}^2$ ) and group III (blue) all the other larger streams. Panel a displays scatter plots of reach-scale mean daily GPP, ER and NEP against drainage area, in logarithmic scale, and their piece-wise regression lines whose equations read as follows (lbp = left side; rbp = right site of the break point):  $\text{GPP}_{\text{lbp}} = 0.779 - 0.027 \log(A)$ ;  $\text{GPP}_{\text{rbp}} = -1.264 + 0.676 \log(A)$ ;  $\text{ER}_{\text{lbp}} = -2.43 + 0.270 \log(A)$ ;  $\text{ER}_{\text{rbp}} = -0.59 - 0.207 \log(A)$ ;  $\text{NEP}_{\text{lbp}} = -651 + 0.240 \log(A)$ ;  $\text{NEP}_{\text{rbp}} = -2.712 + 0.649 \log(A)$ . Breakpoints have been selected to minimize the overall RMSE among all possible combinations (including no breakpoints). Panel b displays the contribution of the different groups to the total, network-scale GPP and ER, expressed per unit of streambed area of the entire river network. Bottom plot of panel b shows network scale NEP per unit of river network streambed area. Top row of panel c shows the frequency distribution of the Strahler's order of the streams belonging to the three different groups. Bottom plots show the range of variability (colored areas) and the average trend (black lines) of the reach-scale GPP, ER, and NEP of the three different groups.

# **Ecosystem metabolism and restoration**

# The influence of floodplain restoration on whole-stream metabolism in an agricultural stream: insights from a 5-year continuous data set

Sarah S. Roley<sup>1,3</sup>, Jennifer L. Tank<sup>1,4</sup>, Natalie A. Griffiths<sup>1,5</sup>, Robert O. Hall Jr.<sup>2,6</sup>, and Robert T. Davis<sup>1,7</sup>

## Restoration and stream metabolism

- From an incised channel to a wider channel with floodplains
- Implications for hydraulic geometry

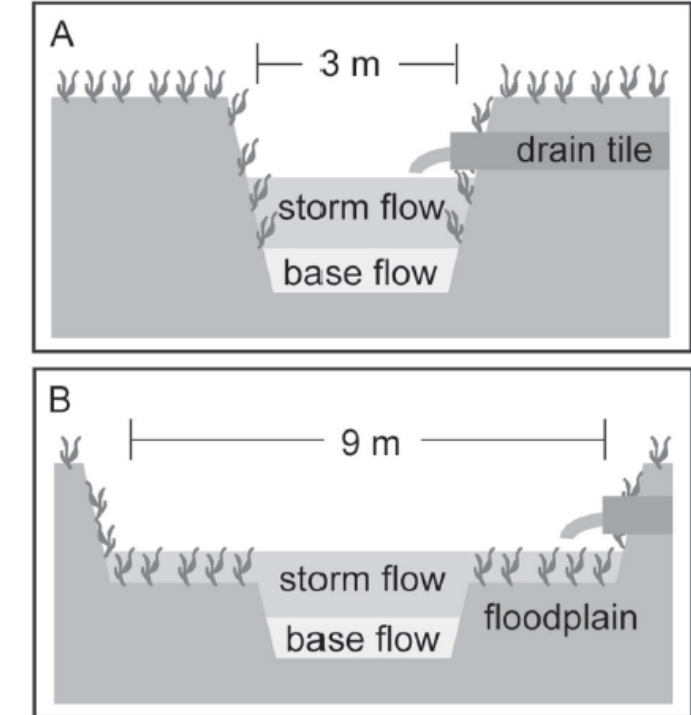


Figure 1. A.—A conventional agricultural ditch. B.—A 2-stage ditch, with floodplains added. Note that the baseflow channel dimensions did not change.

# The influence of floodplain restoration on whole-stream metabolism in an agricultural stream: insights from a 5-year continuous data set

Sarah S. Roley<sup>1,3</sup>, Jennifer L. Tank<sup>1,4</sup>, Natalie A. Griffiths<sup>1,5</sup>, Robert O. Hall Jr.<sup>2,6</sup>, and Robert T. Davis<sup>1,7</sup>

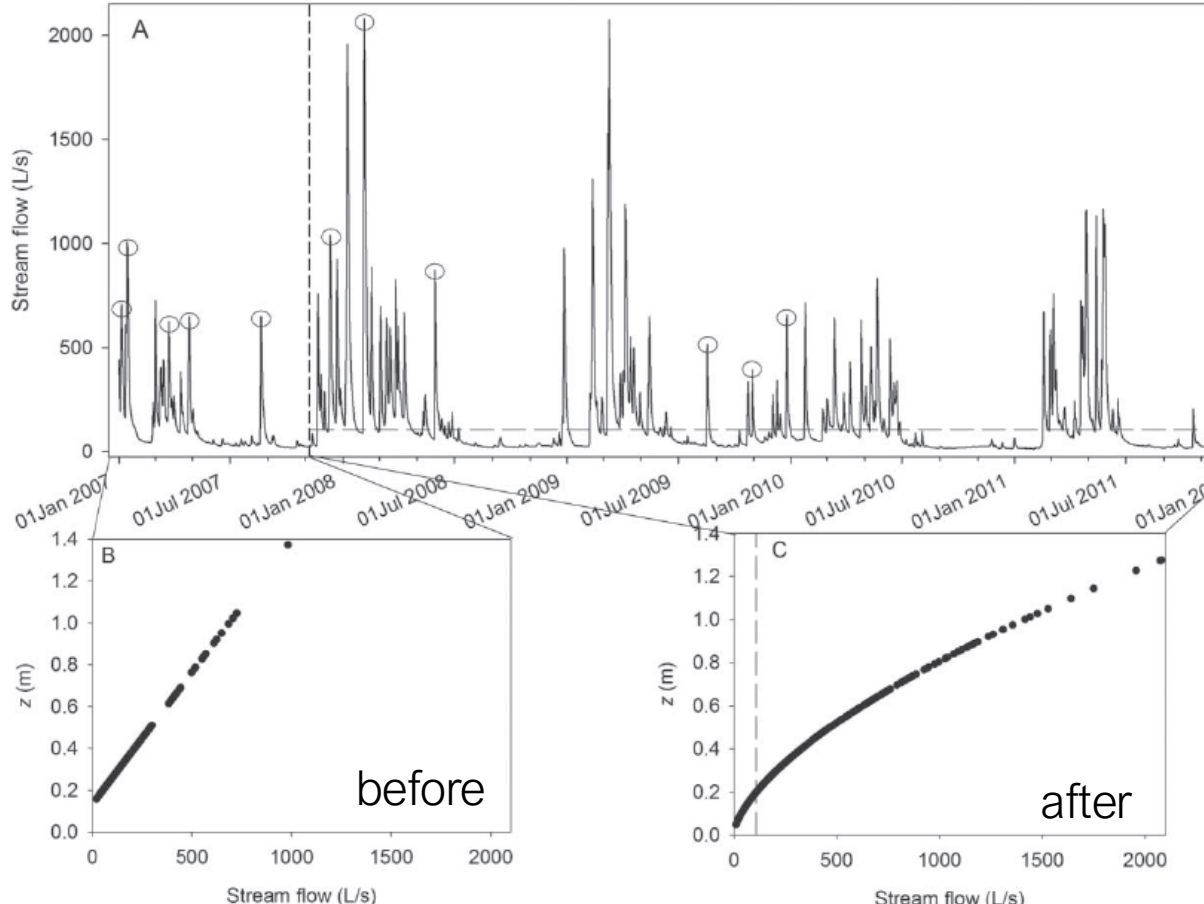


Figure 2. Discharge ( $Q$ ) in the treatment (TRT) reach (A) and the regression relationship between  $Q$  and depth ( $z$ ) before (B) and after (C) restoration. In panel A, the vertical dashed line represents the 2-stage ditch restoration date and circles indicate the storms analyzed for resistance and resilience. The horizontal line in panel A and the vertical line in panel C represent the  $Q$  at which water begins to flow onto the floodplains.

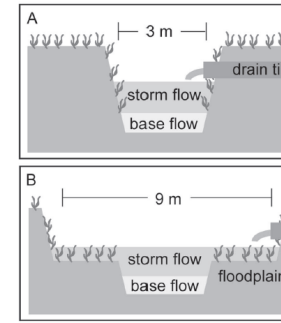


Figure 1. A—A conventional agricultural ditch. B—A 2-stage ditch, with floodplains added. Note that the baseflow channel dimensions did not change.

Restoration changes the relationship between discharge and water depth

# The influence of floodplain restoration on whole-stream metabolism in an agricultural stream: insights from a 5-year continuous data set

Sarah S. Roley<sup>1,3</sup>, Jennifer L. Tank<sup>1,4</sup>, Natalie A. Griffiths<sup>1,5</sup>, Robert O. Hall Jr.<sup>2,6</sup>, and Robert T. Davis<sup>1,7</sup>

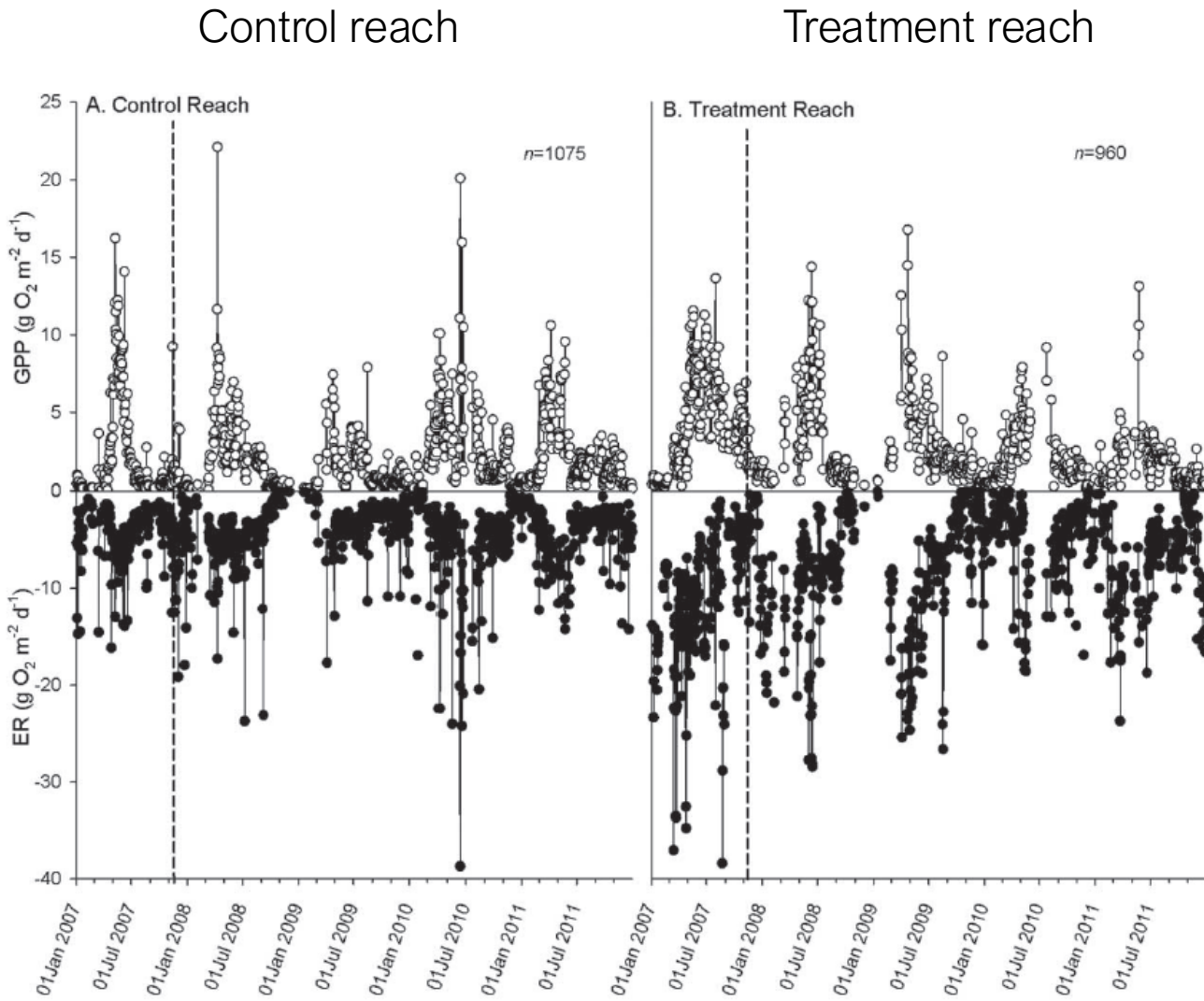


Figure 3. Gross primary production (GPP) and ecosystem respiration (ER) in the control (CTL) (A) and treatment (TRT) (B) reaches. Vertical dashed lines represent the 2-stage ditch restoration date.

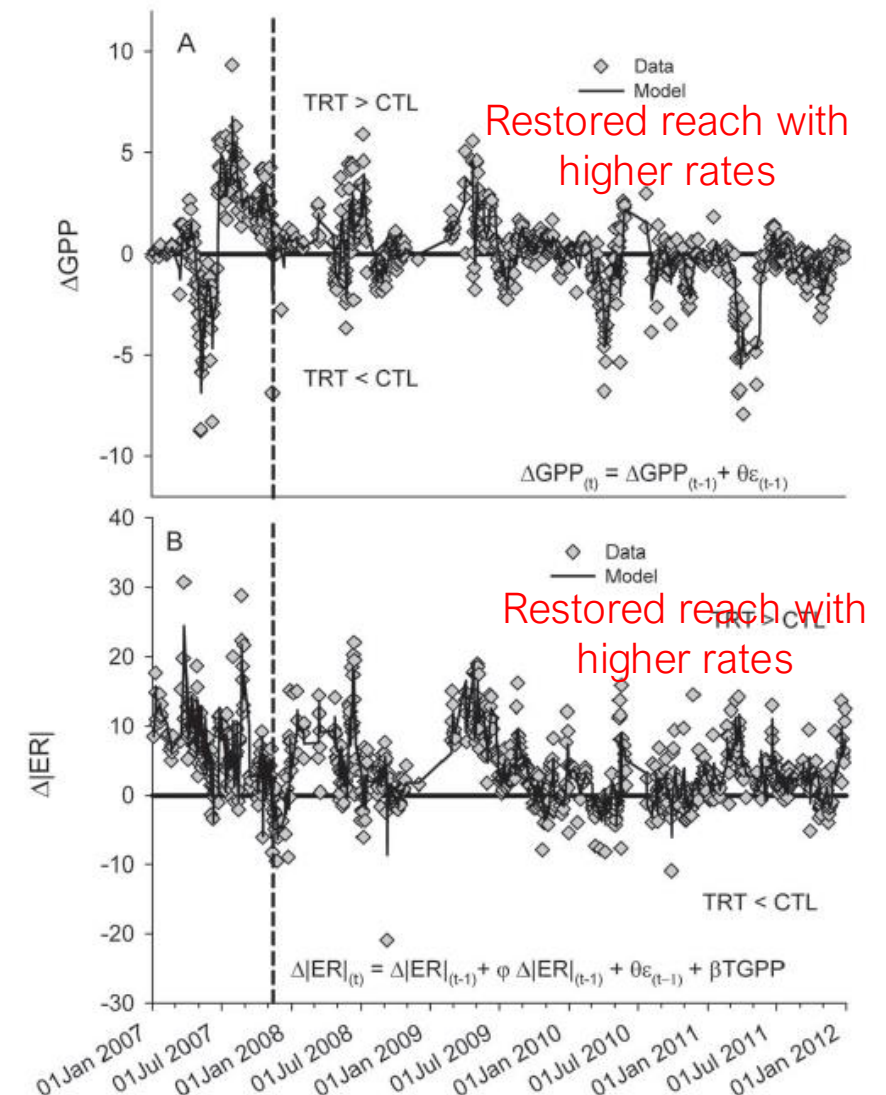
# The influence of floodplain restoration on whole-stream metabolism in an agricultural stream: insights from a 5-year continuous data set

Sarah S. Roley<sup>1,3</sup>, Jennifer L. Tank<sup>1,4</sup>, Natalie A. Griffiths<sup>1,5</sup>, Robert O. Hall Jr.<sup>2,6</sup>, and Robert T. Davis<sup>1,7</sup>

$\Delta GPP$ ,  $\Delta ER$  as difference between treatment (restored) and control (non restored)

Restoration of the channel geomorphology increases ecosystem metabolism, both for ER and GPP.

Figure 5. Difference in gross primary production ( $\Delta GPP$ ) (A) and in ecosystem respiration ( $\Delta |ER|$ ) (B) between the treatment (TRT) and control (CTL) reaches with the results of the best-fit auto-regressive integrated moving average (ARIMA) model. Points that fall above 0 are the dates on which the TRT reach had higher rates, and points that fall below 0 are the dates on which the CTL reach had higher rates. The dashed line represents the restoration date. See Table 2 for regression abbreviations.



The metabolic regimes of flowing waters

E. S. Bernhardt <sup>1,\*</sup> J. B. Heffernan <sup>2</sup> N. B. Grimm <sup>3</sup> E. H. Stanley <sup>4</sup> J. W. Harvey <sup>5</sup>  
M. Arroita, <sup>6,7</sup> A. P. Appling, <sup>8</sup> M. J. Cohen, <sup>9</sup> W. H. McDowell <sup>10</sup> R. O. Hall, Jr., <sup>7,a</sup> J. S. Read, <sup>11</sup>  
B. J. Roberts, <sup>12</sup> E. G. Stets, <sup>13</sup> C. B. Yackulic <sup>14</sup>

# Restoring a stream by constructing a wastewater treatment plant

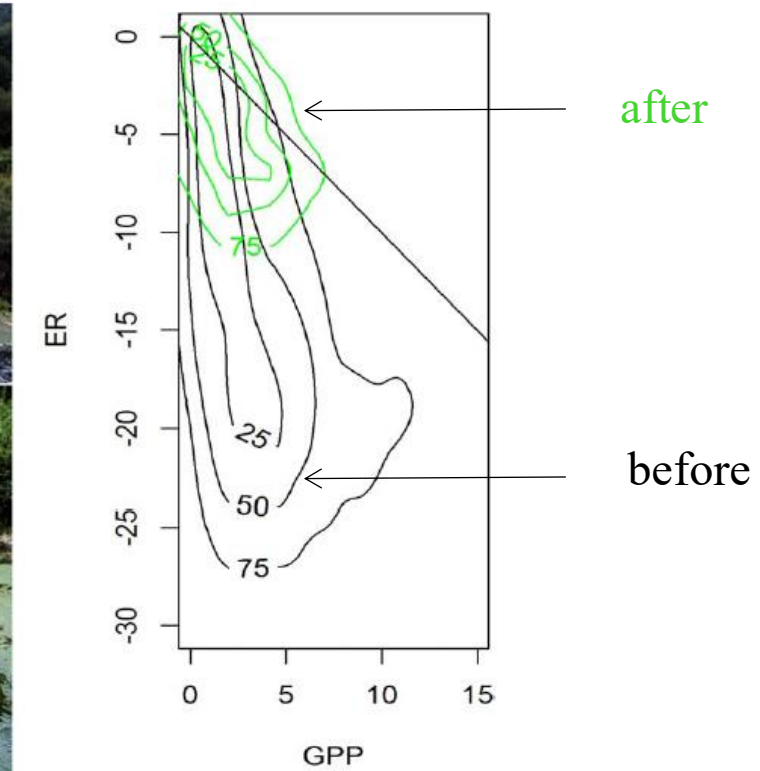


**Fig. 8.** Two photos of the Oria River and its metabolic fingerprint before (black) and after (green) the construction of a wastewater treatment plant. Photo credits to M. Arroita and A. Elosegi. [Color figure can be viewed at [wileyonlinelibrary.com](http://wileyonlinelibrary.com)]

Twenty years of daily metabolism show riverine recovery following  
sewage abatement

Maite Arroita,<sup>1,2\*</sup> Arturo Elosegi,<sup>1</sup> Robert O. Hall Jr.<sup>2</sup>

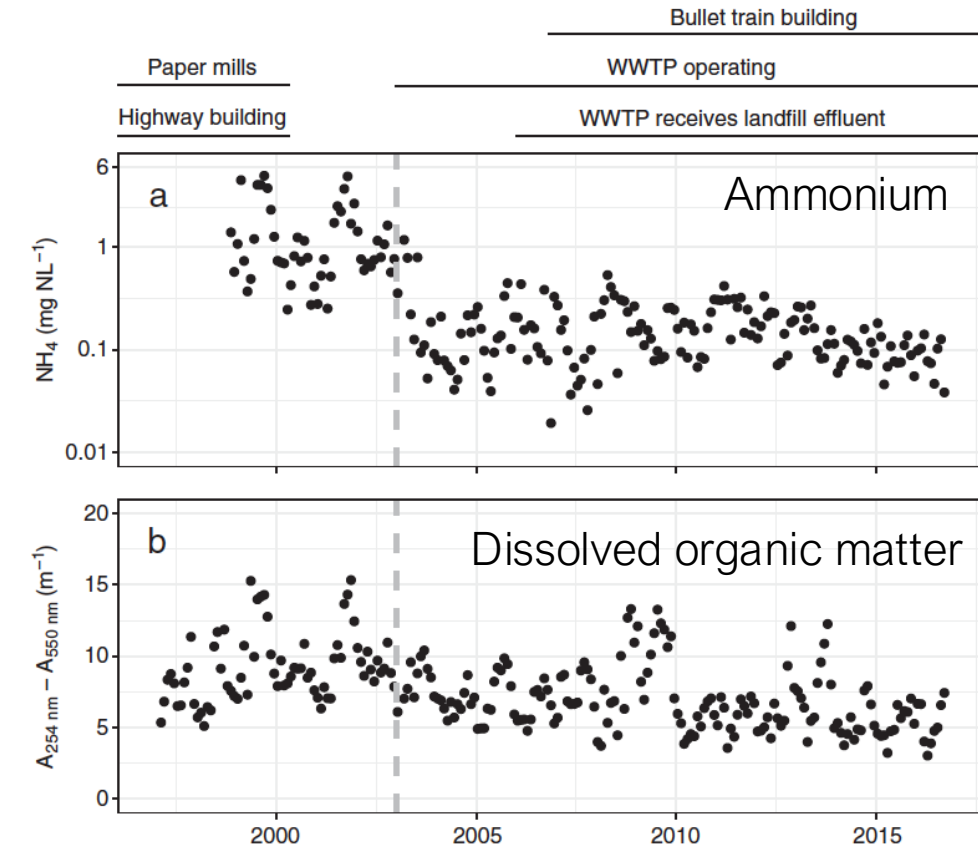


**Fig. 1.** Monthly means of ammonium ( $\text{NH}_4$ ) concentration (a) and DOM absorbance (b;  $A_{254\text{nm}} - A_{550\text{nm}}$ ; proxy for DOM concentration) declined following waste water treatment plant installation (dashed gray line). Note log scale for  $\text{NH}_4$ .

Twenty years of daily metabolism show riverine recovery following sewage abatement

Maite Arroita,<sup>1,2\*</sup> Arturo Elosegi,<sup>1</sup> Robert O. Hall Jr.<sup>2</sup>

GPP summer peaks decreased

ER decreased over the entire year

Less heterotrophic ecosystem

Gas exchange rate increased (absence of algal mats and increasing turbulence)

Improved aeration

Higher fish biodiversity

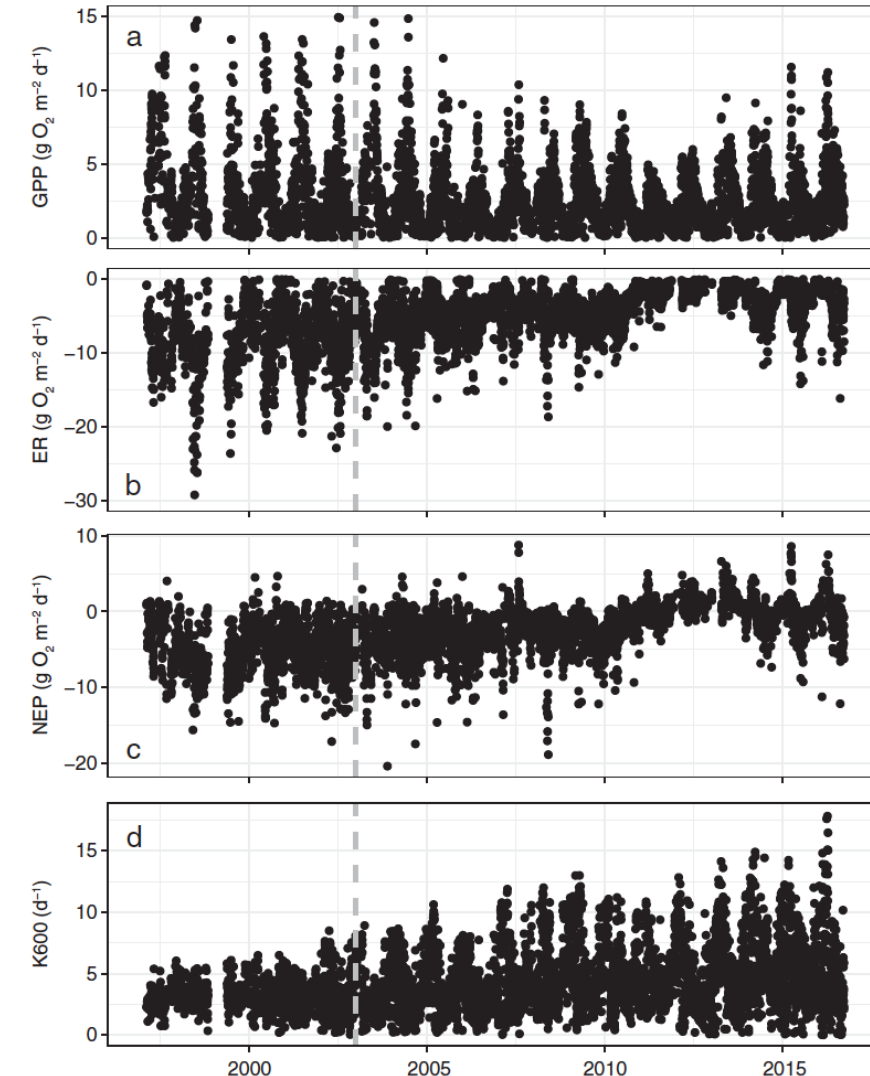


**Fig. 2.** Following waste water treatment plant installation (dashed gray line) GPP (a) and ER (b) gradually decreased, NEP shifted from highly heterotrophic to a balance between GPP and ER (c), and gas exchange rate coefficient (K600) gradually increased (d).

# Ecosystem engineers and metabolism



# Ecosystem engineering and subsidies

- Resuspension of fine sediments
- Bedform alteration



- Nutrient and organic matter amendment
- with marine-derived C N P

# Whole-Stream Metabolism Responds to Spawning Pacific Salmon in Their Native and Introduced Ranges



# Whole-Stream Metabolism Responds to Spawning Pacific Salmon in Their Native and Introduced Ranges

Salmon spawning and biomass stimulate stream ecosystem metabolism

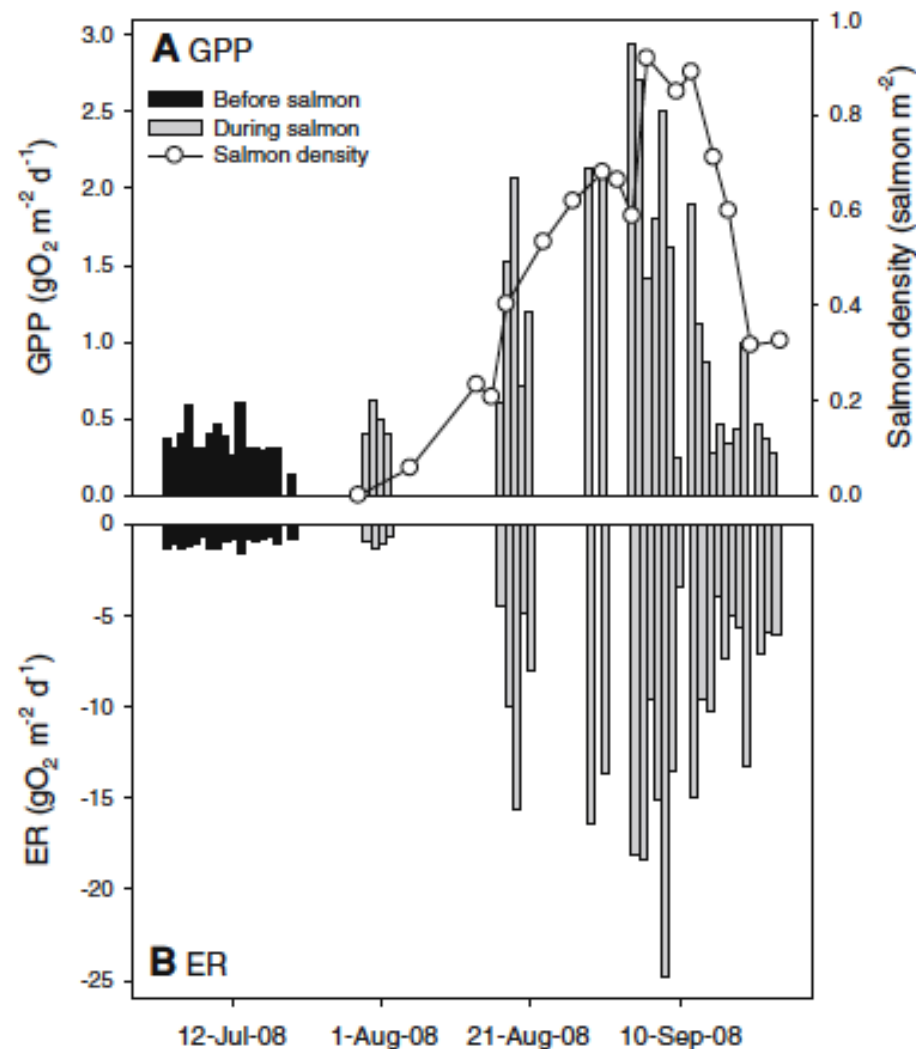


**Figure 3.** Semi-continuous **A** GPP and **B** ER before and during the salmon run in Twelve-Mile Creek in 2008, including salmon density (circle). ER, representing the consumption of oxygen, is displayed as negative values to provide contrast with concurrent GPP.

# Whole-Stream Metabolism Responds to Spawning Pacific Salmon in Their Native and Introduced Ranges

- Nutrient concentrations increase with salmon spawning (e.g., through increased mortality)
- Promote GPP and ER

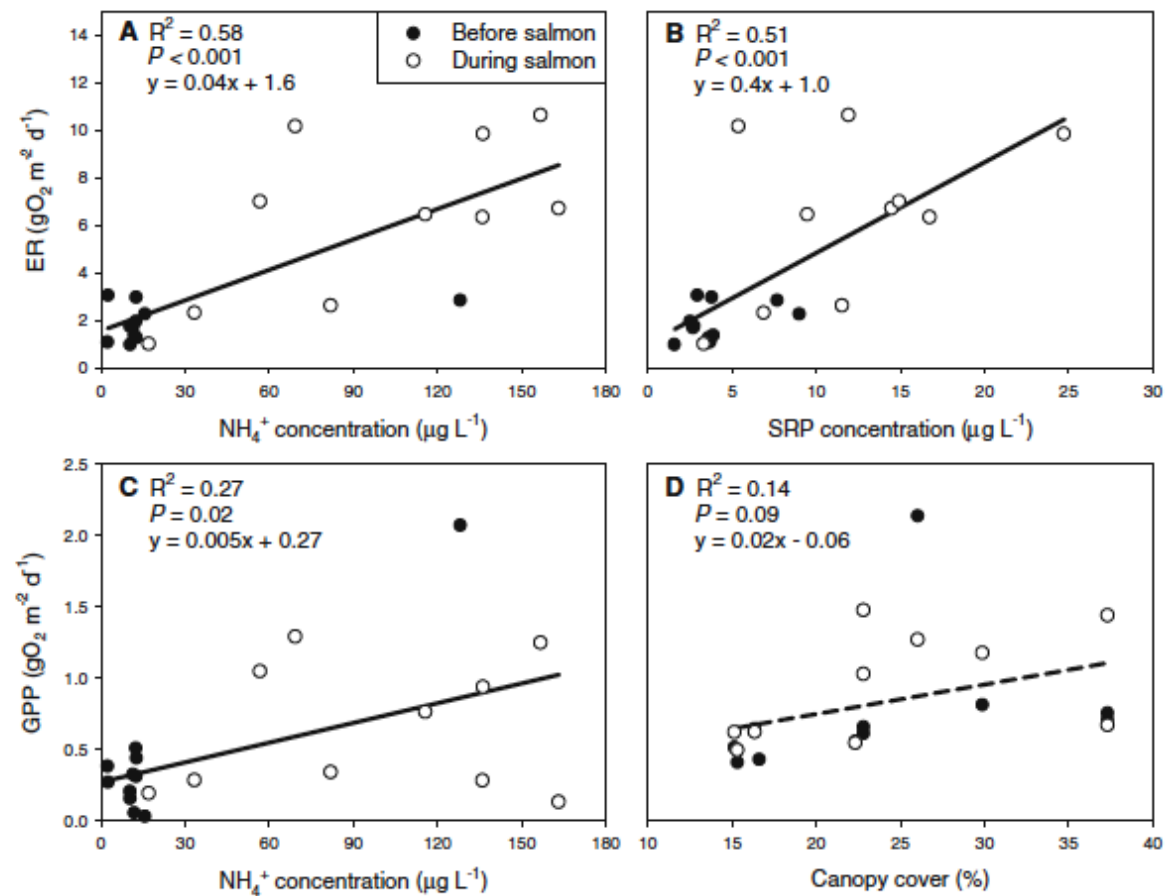


**Figure 6.** Simple linear regressions depicting the dominant controlling variables on ER and GPP. For ER, variation among 11 stream-years was influenced by **A**  $\text{NH}_4^+$  and **B** SRP concentrations, which were both correlated to salmon density. For GPP, variation was influenced by **C**  $\text{NH}_4^+$  concentration and **D** percent open canopy. Data used in the analyses include ER and GPP from before (filled circle) and during (white circle) the salmon run in Southeast Alaska and Michigan.

## BIOTIC CONTROL OF STREAM FLUXES: SPAWNING SALMON DRIVE NUTRIENT AND MATTER EXPORT

JONATHAN W. MOORE,<sup>1,4</sup> DANIEL E. SCHINDLER,<sup>2</sup> JACKIE L. CARTER,<sup>2</sup> JUSTIN FOX,<sup>3</sup> JENNIFER GRIFFITHS,<sup>2</sup> AND GORDON W. HOLTGRIEVE<sup>1,5</sup>

<sup>1</sup>Biology Department, Box 351800, University of Washington, Seattle, Washington 98195 USA

<sup>2</sup>School of Aquatic and Fishery Sciences, Box 350220, University of Washington, Seattle, Washington 98195 USA

<sup>3</sup>Center for Limnology, University of Wisconsin, Madison, Wisconsin 53706 USA

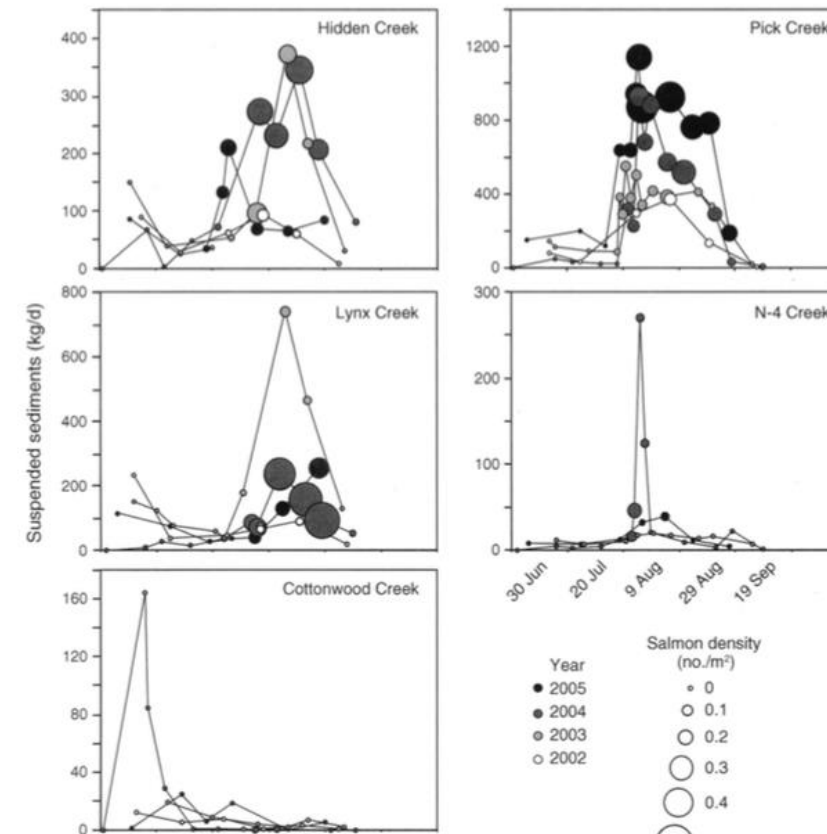


FIG. 1. Seasonal flux of suspended sediments (dry mass) from streams across all years. Shown are streams with three or more years of data. Circle size is proportional to the density of live sockeye salmon in the stream on the day of that sampling. The largest circles correspond to densities of 0.5 salmon/m<sup>2</sup>, while the smallest circles represent 0.0 salmon/m<sup>2</sup>. Symbol fill corresponds to year. Notice that the y-axes have different scales. We examined the impacts of sockeye salmon on ecosystem fluxes of streams located within the Wood River drainage of southwestern Alaska, USA.

Bioturbation and excretion increase downstream nutrient and particle export from headwaters — downstream impacts, but.....

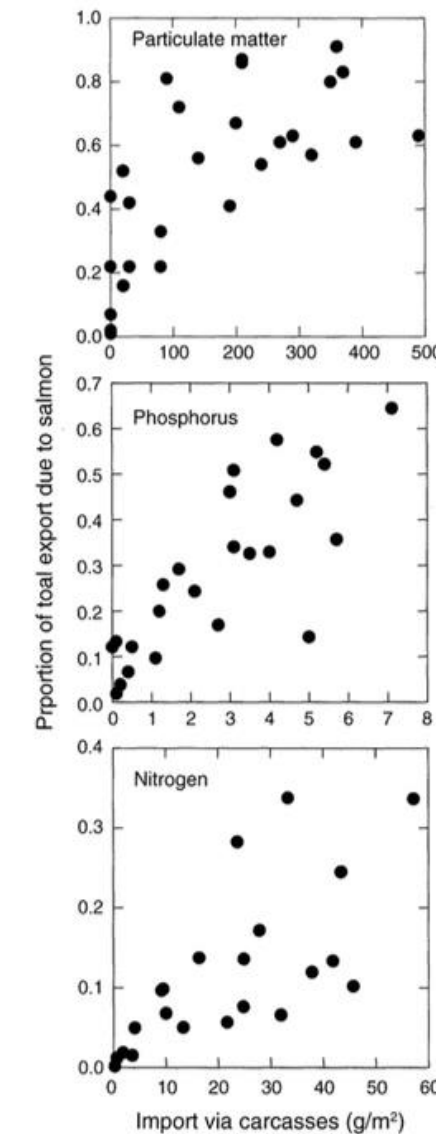
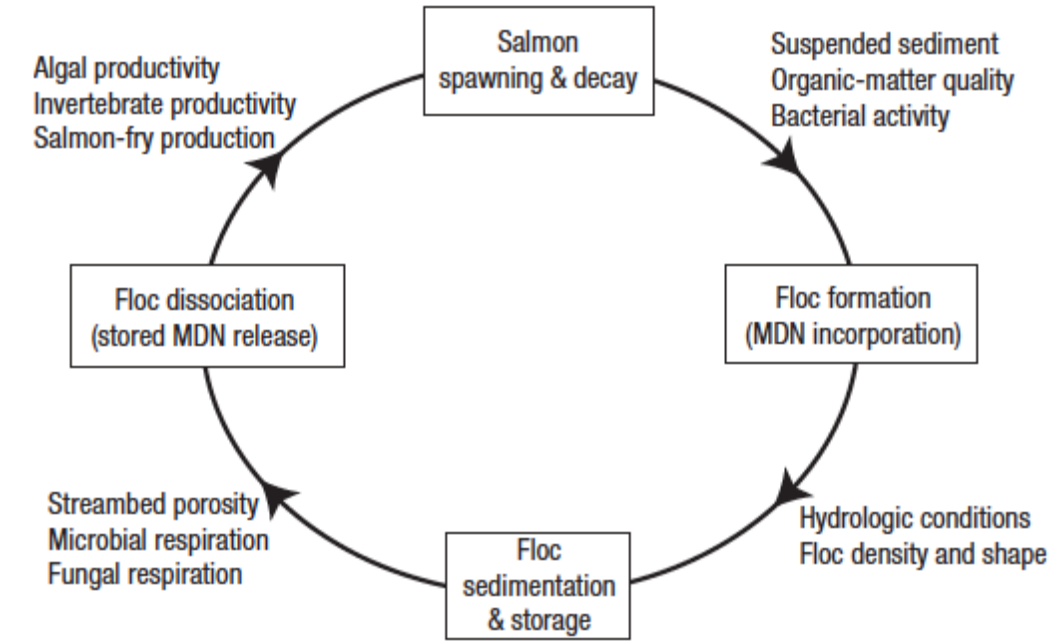


FIG. 7. Relative importance of bioturbation and other salmon activities (excretion) in export of nutrients and matter. Each point is a stream-year, the proportion of the total export that was attributed to salmon activities, plotted as a function of salmon density (import of nutrient and matter by carcasses).

## Delivery of marine-derived nutrients to streambeds by Pacific salmon

JOHN F. REX\* AND ELLEN L. PETTICREW

- Mineral particles aggregate with salmon-derived OM
- Organo-mineral complexes settle
- Enter the sediments via advective transport (links back to sediment clogging)
- “Fertilize” the sedimentary environment
- Supports primary production
- Subsidizes the stream food web
- Provides energy/nutrient to juvenile salmon



**Figure 1** The salmon-floc feedback loop. The model presented includes factors that may regulate each stage (boxes) of the loop during the delivery and cycling of marine-derived nutrients (MDN) in natal Pacific salmon streams.

# Marine derived nitrogen enters the stream food web?

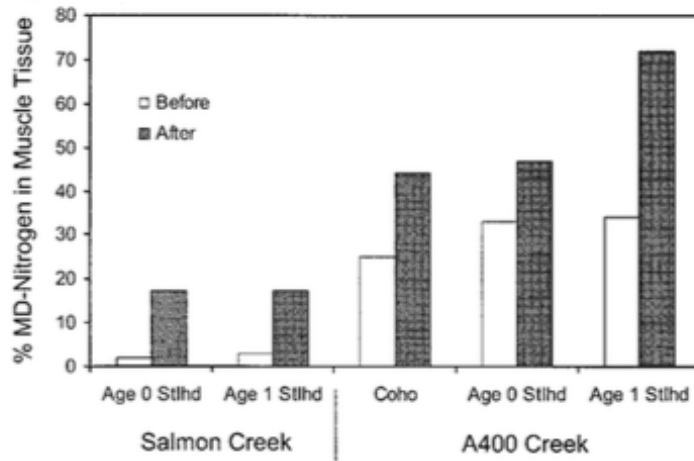


Figure 2. Increase in the proportion of salmon-derived N in the dorsal muscle of juvenile steelhead and salmon in two streams in southwestern Washington to which salmon carcasses were added. Before values indicate the proportion prior to addition of carcasses; the after value represents the proportion after carcasses had fully decomposed (about 6 weeks after carcass addition). The proportion of MD-nitrogen was estimated from N stable isotope ratios. The higher pre-addition values at A400 Creek are likely due to the higher abundance of naturally spawning salmon at this site than at Salmon Creek. Data from Bilby and others (1998).

## Adding salmon carcasses:

- Evidence of marine derived nitrogen (MDN) incorporated into the stream food web
- Based in stable isotope signatures

# Keystone Interactions: Salmon and Bear in Riparian Forests of Alaska

James M. Helfield,<sup>1,3\*</sup><sup>†</sup> and Robert J. Naiman<sup>2</sup>

- Marine subsidies of headwater food webs
- Subsidizing terrestrial food webs
- Stimulating vegetation adjacent to streams and rivers

Upstream longitudinal connectivity  
Lateral connectivity (aquatic/terrestrial)

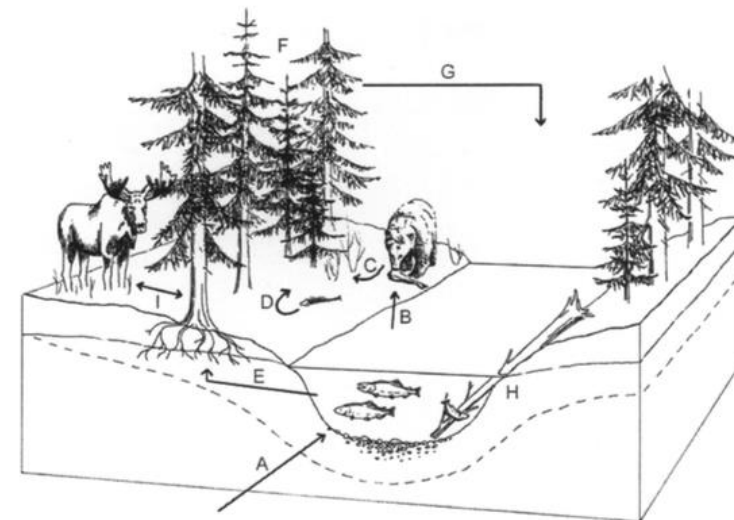


**Figure 4.** Cycling of marine-derived nitrogen (MDN) and effects on river and riparian ecosystems: (A) Spawning salmon transport MDN upstream; (B) Bears and other piscivores consume salmon; (C) Bears and other piscivores disseminate salmon-enriched wastes and partially-eaten salmon carcasses in the riparian forest; (D) Terrestrial and aquatic insects colonize salmon carcasses, enhancing decomposition and MDN diffusion; (E) Dissolved N downwells into hyporheic flowpaths beneath the riparian forest and is taken up by tree roots; (F) MDN inputs enhance foliar N content and growth rates of riparian trees; (G) Riparian trees provide shade, bank stabilization, allochthonous organic matter and large woody debris (LWD), enhancing the quality of instream habitat for salmonid fishes; (H) LWD retains post-spawn salmon carcasses in streams, further enhancing MDN availability; (I) Increased foliar N content enhances palatability and nutrition of riparian plants, potentially altering patterns of browsing, which in turn affects patterns of riparian productivity and species composition.

# Global nutrient transport in a world of giants

Christopher E. Doughty<sup>a,1</sup>, Joe Roman<sup>b,c</sup>, Søren Faurby<sup>d</sup>, Adam Wolf<sup>e</sup>, Alifa Haque<sup>a</sup>, Elisabeth S. Bakker<sup>f</sup>, Yadvinder Malhi<sup>a</sup>, John B. Dunning Jr.<sup>g</sup>, and Jens-Christian Svenning<sup>d</sup>

<sup>a</sup>Environmental Change Institute, School of Geography and the Environment, University of Oxford, Oxford OX1 3QY, United Kingdom; <sup>b</sup>Organismic and Evolutionary Biology, Harvard University, Cambridge, MA 02138; <sup>c</sup>Gund Institute for Ecological Economics, University of Vermont, Burlington, VT 05445; <sup>d</sup>Section of Econometrics & Biodiversity, Department of Bioscience, Aarhus University, DK-8000 Aarhus C, Denmark; <sup>e</sup>Department of Ecology and Evolutionary Biology, Princeton University, Princeton, NJ 08544; <sup>f</sup>Department of Aquatic Ecology, Netherlands Institute of Ecology, 6708 PB Wageningen, The Netherlands; and <sup>g</sup>Department of Forestry and Natural Resources, Purdue University, West Lafayette, IN 47907

2015, PNAS

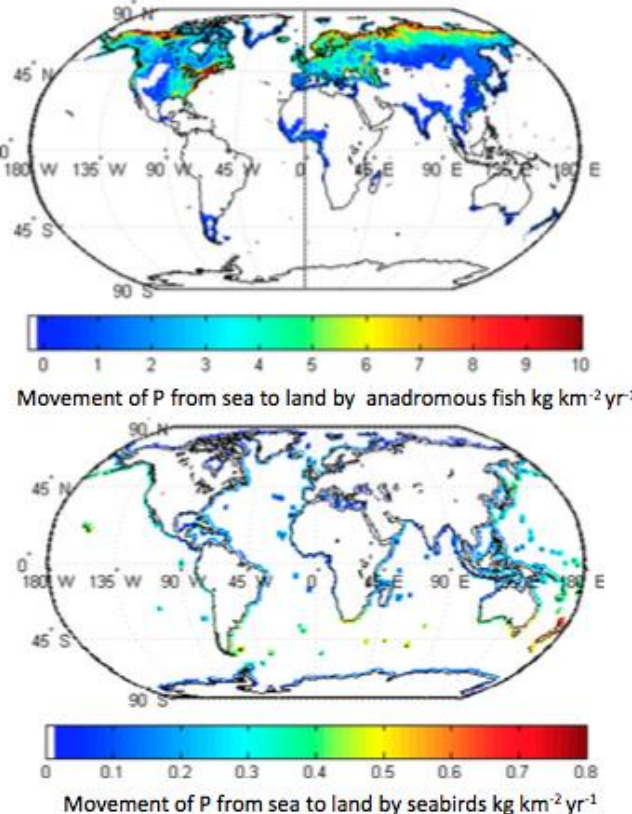


**Fig. 3.** Nutrient movement of P from ocean to land by anadromous fish and seabirds. (Top) Global estimates of historical P ( $\text{kg km}^{-2} \text{yr}^{-1}$ ) moved by the bodies of anadromous fish in the past. Nutrient movement by anadromous fish may be underestimated in tropical regions due to a lack of data. (Bottom) Global estimates of guano movement to coastal land by all seabirds, assuming 20% of the guano arrives on land (measured in  $\text{kg km}^{-2} \text{yr}^{-1}$ ) and assuming theoretical population densities of seabirds based on body mass population density scaling relationships (43).

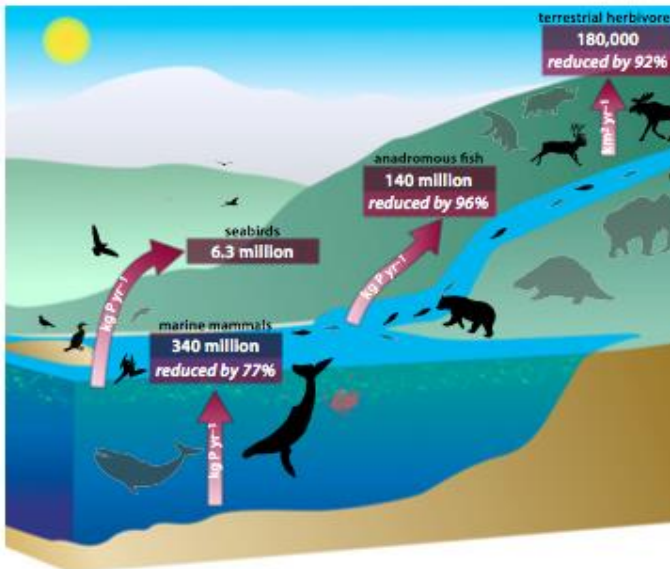
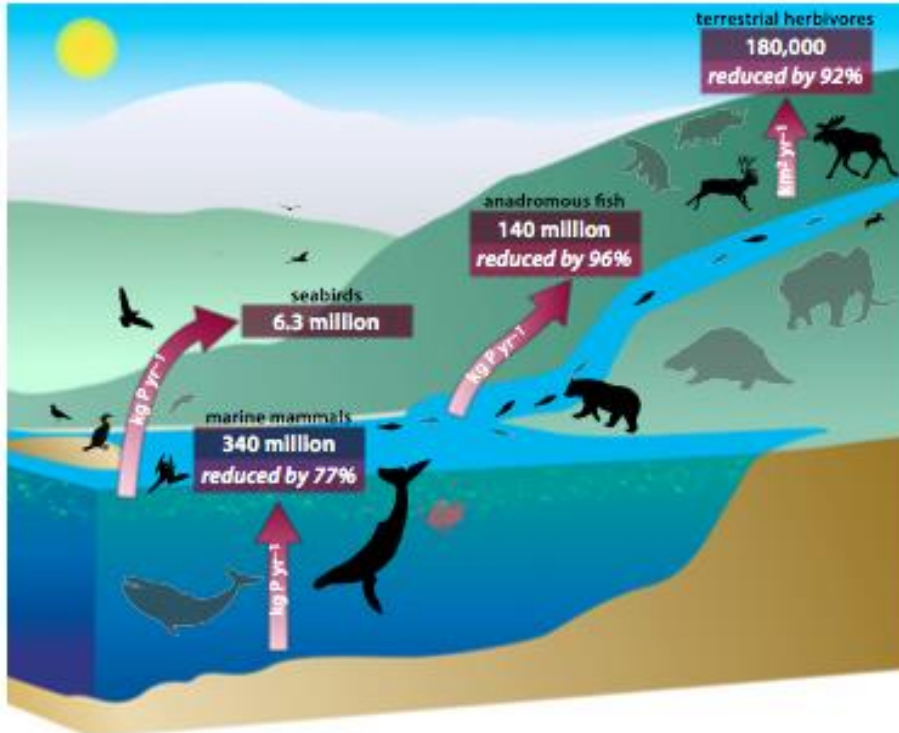


**Fig. 4.** Potential interlinked system of recycling nutrients. The diagram shows a potential route of nutrient transport of the planet in the past. Red arrows show the estimated fluxes or diffusion capacity of nutrients listed in Table 1. Grey animals represent extinct or reduced population densities of animals.

- Migrating salmons convey nutrients from the ocean to the headwater streams
- Anadromous fish important nutrient (notably phosphorus) conveyors from the ocean to the headwaters

Imagine all the dams that inhibit the migration of salmon and other fish to spawn, 'engineer' and fertilize headwaters with marine or lake-derived matter and nutrients...



All connected  
...metabolism and nutrient cycling

Breaking the continuum

- Ecosystem health
- Economy, fisheries, social structures